ORNL/TM-12028

ornl

OAK RIDGE NATIONAL LABORATORY

MARTIN MARIETTA

Determination of Neutron Dose from Criticality Accidents with Bioassays for Sodium-24 in Blood and Phosphorus-32 in Hair

Y. Feng
K. S. Brown
W. H. Casson
G. T. Mei
L. F. Miller
M. Thein

MANAGED BY
MARTIN MARIETTA ENERGY SYSTEMS, INC.
FOR THE UNITED STATES
DEPARTMENT OF ENERGY

ORNL/TM-12028

Office of Radiation Protection

DETERMINATION OF NEUTRON DOSE FROM CRITICALITY ACCIDENTS WITH BIOASSAYS FOR SODIUM-24 IN BLOOD AND PHOSPHORUS-32 IN HAIR

Y. Feng
K. S. Brown
W. H. Casson
G. T. Mei
L. F. Miller
M. Thein

Manuscript Completed—March 1993

Date Published—June 1993

Prepared by the
Oak Ridge National Laboratory
Oak Ridge, Tennessee 37831-6285
managed by
MARTIN MARIETTA ENERGY SYSTEMS, INC.
for the
U.S. DEPARTMENT OF ENERGY
under contract DE-AC05-84OR21400

DE F 1332.15
3-93)
ombines previous
rsion of DOE
1332.15 and .16.
other editions are
solete.

U. S. DEPARTMENT OF ENERGY
RECOMMENDATIONS FOR THE ANNOUNCEMENT AND DISTRIBUTION OF DEPARTMENT OF ENERGY (DOE) SCIENTIFIC AND TECHNICAL INFORMATION (STI)

(See instructions on reverse side. Use plain bond paper if additional space is needed for explanations.)

OMB Control No
1910-1400
OMB Burden
Disclosure
Statement on
reverse side

ART I *(DOE, DOE Contractors, Grantees, and Awardees complete)*

A. Product/Report Data

1. (Award) Contract No. DE-AC05-84OR21400

2. Title Determination of Neutron Dose from Criticality Accidents with Bioassays for Sodium-24 in Blood and Phosphorus-32 in Hair

3. Product/Report Description

☒ a. Report *(Complete all that apply)*
- (1) ☒ Print ☐ Nonprint *(specify)*
- (2) ☐ Quarterly ☐ Semiannual ☐ Annual ☐ Final
- ☒ Topical ☐ Phase I ☐ Phase II
- ☐ Other *(specify)*

Dates covered _____ thru _____

☐ b. Conference/Meeting/Presentation *(Complete all that apply)*
- (1) ☐ Print ☐ Nonprint *(specify)*
- ☐ Published proceedings
- ☐ Other *(specify)*
- (2) Conference Title *(no abbreviations)*

Location *(city/state/country)*

Date(s) *(m/d/y)* / / thru *(m/d/y)* / /

Sponsor

☐ c. Software—Additional forms are required. Follow instructions on the back of this form.

☐ d. Other *(Provide complete description)*

B. Patent Information

Yes	No	
☐	☒	Is any new equipment, process, or material disclosed? If yes, identify page numbers
☐	☒	Has an invention disclosure been submitted? If yes, identify the disclosure number and to whom it was submitted. Disclosure number / Submitted to
☐	☒	Are there patent-related objections to the release of this STI product? If so, state the objections.

C. Contact *(Person knowledgeable of content)*

Name
Phone
Position
Organization

ART II *(DOE/DOE Contractors complete/or as instructed by DOE contracting officer)*

A. DOE Identifiers

. Product/Report Nos. ORNL/TM-12028

. Funding Office(s) *(NOTE: Essential data)* 27 38 03 00 0

B. Copies for Transmittal to AD-21 (OSTI)

(STI must be of sufficient quality for microfilming/copying.)

1. One for classified processing
2. *(number)* for standard classified distribution
3. Two unclassified for processing
4. *(number)* for program unclassified distribution
5. UC/C Category 407
6. Additional instructions/explanations

(Do not identify Sigma categories for Nuclear Weapons Data reports, and do not provide additional instructions that are inconsistent with C below.)

C. Recommendation *("X" at least one)*

1. Program/Standard Announcement/Distribution *(Available to U.S. and foreign public)*
2. Classified *(Standard Announcement only)*
3. Special Handling *(Legal basis must be noted below.)*
   - a. Unclassified Controlled Nuclear Information (UCNI)
   - b. Export Control/ITAR/EAR
   - c. Temporary hold pending patent review
   - d. Translations of copyrighted material
   - e. Small Business Innovation Research (SBIR)
   - f. Commercializable information
     - (1) Proprietary
     - (2) Protected CRADA information
       Release date / /
     - (3) Other *(explain)*
4. Program Directed Special Handling *(copy attached)*

D. Releasing Official

A. Patent Clearance *("X" one)*
- ☐ Has been submitted for DOE patent clearance
- ☒ DOE patent clearance has been granted

B. Released by

(Name) D.R. Hamrin
(Signature) D. R. Hamrin (KB)
(Phone) (615) 574-6752
(Date) June 17, 1993

TABLE OF CONTENTS

TABLE OF CONTENTS
(continued)

TABLE OF CONTENTS
(continued)

LIST OF FIGURES

LIST OF FIGURES
(continued)

LIST OF TABLES

ACKNOWLEDGMENTS

The authors wish to express appreciation to J. S. Bogard, D. J. Downing, G. D. Kerr, C. S. Sims, and J. E. Turner at Oak Ridge National Laboratory (ORNL), as well as R. P. Osborne, Radiation Safety Officer at The University of Tennessee—Knoxville (UTK), and Dr. Schwietzer in the Chemistry Department of UTK for their comments, suggestions, and assistance for this research. The authors are grateful to K. H. Galloway, C. J. Franklin and L. R. Pyles (ORNL) for updating this manuscript.

DETERMINATION OF NEUTRON DOSE FROM CRITICALITY ACCIDENTS WITH BIOASSAYS FOR SODIUM-24 IN BLOOD AND PHOSPHORUS-32 IN HAIR

Y. Feng,* K. S. Brown,† W. H. Casson,† G. T. Mei,
L. F. Miller,* and M. Thein

ABSTRACT

A comprehensive review of accident neutron dosimetry using blood and hair analysis was performed and is summarized in this report. Experiments and calculations were conducted at Oak Ridge National Laboratory (ORNL) and the University of Tennessee (UT) to develop measurement techniques for the activity of ^{24}Na in blood and ^{32}P in hair for nuclear accident dosimetry.

An operating procedure was established for the measurement of ^{24}Na in blood using an HPGe detector system. The sensitivity of the measurement for a 20-mL sample is 0.01-0.02 Gy of total neutron dose for hard spectra and below 0.005 Gy for soft spectra based on a 30- to 60-min counting time. The operating procedures for direct counting of hair samples are established using a liquid scintillation detector. Approximately 0.06-0.1 Gy of total neutron dose can be measured from a 1-g hair sample using this procedure. Detailed procedures for chemical dissolution and ashing of hair samples are also developed.

A method is proposed to use blood and hair analysis for assessing neutron dose based on a collection of 98 neutron spectra. Ninety-eight blood activity-to-dose conversion factors were calculated. The calculated results for an uncollided fission spectrum compare favorably with previously published data for fission neutrons. This nuclear accident dosimetry system makes it possible to estimate an individual's neutron dose within a few hours after an accident if the accident spectrum can be approximated from one of 98 tabulated neutron spectrum descriptions. If the information on accident and spectrum description is not available, the activity ratio of ^{32}P in hair and ^{24}Na in blood can provide information related to the neutron spectrum for dose assessment.

1. INTRODUCTION

1.1 DEFINITION OF NUCLEAR CRITICALITY ACCIDENT

A criticality accident is defined as "an unplanned or uncontrolled nuclear excursion resulting from the assembly of a quantity of fissile material. In some cases the mass of the material may

*University of Tennessee, Knoxville, Tennessee.

†Health and Safety Research Division, Oak Ridge National Laboratory, Oak Ridge, Tennessee.

have a sufficient excess of reactivity to become prompt-critical and result in a very fast pulse of energy accompanied by a field of thermal and ionizing radiation."[1] Despite advanced technology and administrative controls aimed at preventing criticality accidents, the possibility exists that workers and the public could be exposed to radiation emanating from a criticality accident. Approximately 36 separate criticality accidents were reported between 1945 and 1982. The majority occurred before 1964; 13 occurred in the United States.

When a criticality accident occurs, immediate attention must be given to victims receiving integral absorbed doses of greater than 0.25 Gy to a major organ group or the entire body. Fatalities usually occur from exposures above ~2.0 Gy. Fatality is probably inevitable at a dose level of 8.0 Gy.[2] Rapid dose assessment must be provided following a criticality accident to permit medical staff to determine treatment methods for each victim. Use of necessary procedures and facilities for dealing with such incidents is called the accident dosimetry system.

1.2 CHARACTERISTICS OF AN ACCIDENT DOSIMETRY SYSTEM

Criticality accidents present a number of dosimetry problems differing markedly from those encountered in routine personnel dosimetry. Characteristics of criticality accidents include

1. a very low probability of occurrence;
2. a complex spectrum of radiation due to the mixture of neutrons and gammas;
3. a neutron spectrum which varies markedly depending on the type of critical assembly, moderator and shielding material;
4. extremely high intensity of initial radiation; and
5. acute exposure to gamma and neutron radiation.

The use of a dose equivalent is applicable to low-level chronic exposures but would not apply to acute radiation exposure after a criticality accident. Instead, exposure from a nuclear accident should be quantified as the absorbed dose to the body (Gy). In addition, the accident dosimetry system should permit an initial dose determination to be completed within 48 h with an uncertainty of less than 50%, falling to less than 25% within 1 week of the accident.[1]

1.3 TYPES OF ACCIDENT DOSIMETRY SYSTEMS

Nuclear accident dosimetry systems fall into the following categories:

1. personnel dosimeters worn on the body including activation and fission detectors, nuclear track detectors for neutron measurement, and thermoluminescent dose meters (TLDs) for gamma measurement;
2. area dosimeters installed in the general vicinity where a criticality accident could occur; and
3. activation of body components such as whole-body sodium, blood sodium, and phosphorus in hair by neutrons.

The installed area dosimetry system only provides accurate spectral information for the scene of the accident if the system covers the entire area and only one excursion occurs. A simple personnel dosimeter only indicates the dose received by the individual if the orientation of the

person to the critical system at the time of the accident is known. It is possible that the individual may not even be wearing a dosimeter when an accident occurs. When incomplete information about the event or individual exposure is available, body activation may provide the most accurate measurement of the neutron dose received by an individual in an accident.

1.4 OVERVIEW OF PREVIOUS WORK IN BODY ACTIVATION

Use of body activation to determine induced neutron dose in irradiated personnel was first implemented by Hempelmann and associates in 1952.[3] Los Alamos Scientific Laboratory, ORNL, the Atomic Energy Research Establishment (AERE) of the United Kingdom, the International Atomic Energy Agency (IAEA), and other organizations conducted experiments in body activation in the 1960s and 1970s. The mechanisms of body activation by neutrons were developed. Experiments were conducted on phantoms using several different simulated critical assemblies. One of the important contributions from this research is the concept of body capture probability, which accounts for body moderation to the incident neutrons.

Research in accident neutron dosimetry was limited to a certain degree by a lack of information on accident neutron spectra. In the early 1980s, progress in this field was slowed by lessened research emphasis on criticality accidents. Research work on criticality accidents was increased slightly after the Chernobyl accident in the U.S.S.R. in 1986. New and more advanced nuclear measurement equipment has been recently developed which has application to accident dosimetry. In 1990, the IAEA published more detailed information for different calibration neutron spectra and detector responses.[4]

1.5 RESEARCH OBJECTIVES

Department of Energy (DOE) Order 5480.11 requires DOE contractors to establish standards and conduct programs to protect workers from ionizing radiation. ORNL employs an updated nuclear accident dosimetry system, which includes the following elements:[5]

1. a method to conduct initial "screening" of personnel involved in nuclear accidents to determine if they have received significant radiation exposure;
2. methods for analysis of biological materials (including ^{24}Na activity in blood and ^{32}P activity in hair);
3. a system of fixed units capable of yielding estimated radiation doses and the approximate neutron spectra at their fixed locations;
4. personnel dosimeters capable of furnishing sufficient information to determine neutron and gamma doses and/or dose equivalents; and
5. counting facilities to evaluate personnel dosimeters, sodium in blood, and phosphorus in hair.

The objectives of this research are to review the principles of accident neutron dosimetry using bioassay materials (blood and hair), to establish laboratory measurement procedures of ^{24}Na in blood and ^{32}P in hair by neutron activation, and to recommend a practical and rapid accident neutron dose assessment process using blood and hair for the accident dosimetry system at ORNL. The following detailed tasks have been identified to accomplish these objectives:

1. review the previous work on accident neutron dosimetry;
2. study the principles used in experimental facilities for research of this type;
3. conduct experiments to develop suitable methods for hair sample treatment;
4. establish measurement procedures for activation of ^{24}Na in blood by neutrons;
5. establish measurement procedures for activation of ^{32}P in hair by high energy neutron induction;
6. determine the sensitivities of the two established measurement procedures;
7. recommend an accident neutron dosimetry system which can quickly access neutron doses from activated blood and hair without detailed knowledge of the accident neutron spectrum; and
8. analyze the qualitative factors affecting the accident neutron dose determination.

1.6 RESEARCH RESULTS

This research has resulted in accurate documentation of blood and hair activation analysis techniques for an accident neutron dosimetry system at ORNL. Procedures for both blood and hair analysis include sample preparation, material and equipment requirements, preparation of the detection system, activity analysis methods, and requirements of the Minimum Detectable Activity (MDA). Although it is very difficult to obtain detailed and accurate information about the radiation spectrum shortly after an accident, activation of blood and hair is a strong indicator of neutron spectra. This dosimetry system can be used with or without detailed information on the accident neutron spectrum. Activity-to-dose conversion factors based upon referencable open literature sources are calculated for 98 neutron spectra which encompass the most likely neutron spectra expected to be encountered in criticality accidents. Calculated activity ratios between hair and blood can be used to select the most appropriate accident spectrum. In addition, computer codes developed for this research could be useful for data processing in a real accident.

1.7 ORGANIZATION OF THE REPORT

This report is presented in five sections and five appendices. Following the Introduction, the development of measurement procedures for ^{24}Na in blood is addressed in Sect. 2. A description of the experimental facility and measurement system used for this study is included, and the discussion of MDA is also presented in Sect. 2. A similar discussion of ^{32}P in hair is given in Sect. 3, in addition to pretreatment methods for hair samples. Section 4 describes the development of the dosimetry system and the methodology for calculating the 98 blood activity-to-dose conversion factors, in addition to characteristics of hair as a bioassay material in an accident and the qualitative uncertainty of the dosimetry system. Conclusions and suggestions for future research are presented in Sect. 5. The established measurement procedures for ^{24}Na in blood and ^{32}P in hair are presented separately in Appendices A and B. The computer codes developed for this research are presented in Appendix C. Appendix D lists an additional bibliography.

2. DEVELOPMENT OF BLOOD SODIUM MEASUREMENT PROCEDURES

2.1 INTRODUCTION

The human body normally contains about 1.4 g/kg ^{23}Na by weight. The concentration of ^{23}Na in blood is 1.91 mg/mL of blood.[6] Sodium-23 will produce ^{24}Na when it absorbs neutrons. Sodium-24 is a gamma-ray emitter with a 14.8-h radioactive half-life. Sodium-24 decays by emitting a beta particle and two gamma rays having energies of 1.369 and 2.754 MeV. Both blood sodium and body sodium activation can be used as an indication of neutron exposure in an accident.

Measurement of blood sodium is more reliable than the whole-body sodium measurement since whole-body measurement results are affected by the radioactive contamination of the body surface. A NaCl solution was used for this research instead of real human blood.

The blood sodium measurement system, neutron sources, activity counting process, methodology of ^{24}Na activity calculation, and MDA are described in this chapter. The quantities that influence the determination of blood sodium activities are also discussed.

2.2 MEASUREMENT SYSTEM FOR BLOOD SODIUM

Measurement of blood sodium activity is usually made by measuring the gamma activity of small samples of blood. Gamma activities can be measured by a NaI(Tl) crystal scintillator with a multichannel analyzer or by a high-purity germanium (HPGe) detector with a multichannel analyzer.

High-purity germanium is utilized in this research for two reasons. First, most ^{23}Na in the blood occurs in the form of NaCl. When irradiated by neutrons, ^{37}Cl will become ^{38}Cl, and ^{38}Cl is a gamma emitter with a radioactive half-life of 33 min. It has gamma rays of two energies, 1.64 and 2.17 MeV, which are close to gamma-ray energies of ^{24}Na. Most gamma activity in blood during the first 4 h after an excursion is due to ^{38}Cl. A high-energy resolution detector is needed to differentiate between ^{38}Cl and ^{24}Na activity. The resolution of a detector is indicated by the width of its photopeaks. A more narrow peak indicates a greater capacity of the system to distinguish between different gamma rays of closely spaced energies. Energy resolution is defined as the width of a peak halfway between its top and base. High-purity germanium systems have a typical energy resolution of a few tenths of a percentage compared with 5-10% for NaI detectors.

Secondly, HPGe spectrometers used in laboratories for routine measurements are usually routinely calibrated over a broad band of gamma-ray energies under a quality assurance program. Thus, these systems can be immediately utilized after accidents.

2.2.1 Components of Measurement System

A schematic of the measurement system for blood sodium is shown in Fig. 1. The spectrometry system consists of lead shielding, a GMX n-type HPGe detector, a preamplifier,

ORNL-DWG 92M-12970

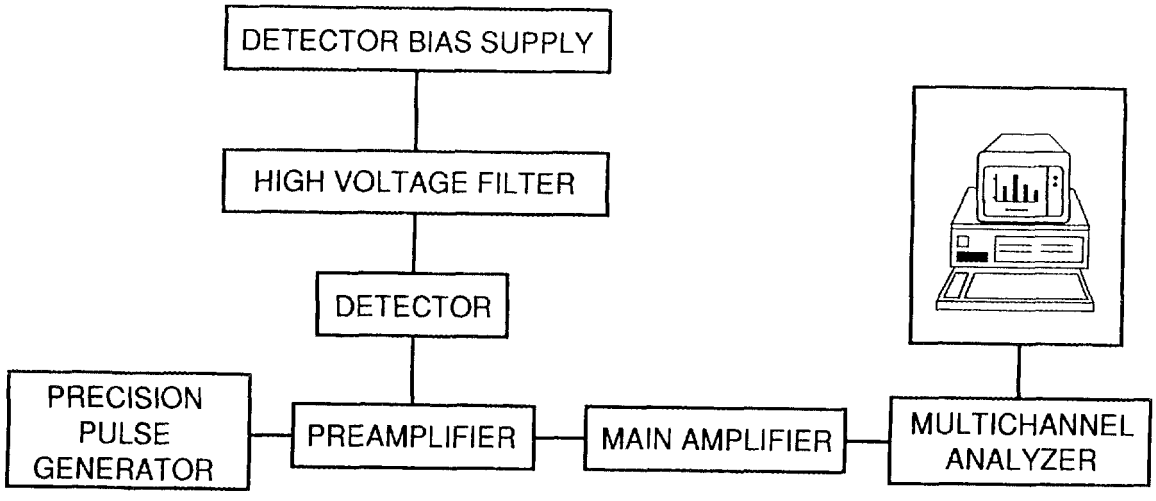

Fig. 1. Schematic showing the measurement system for blood sodium.

a high-voltage filter, a high-voltage bias supply, a main amplifier, and the Advanced Data Collection and Management (ADCAM) System from EG&G ORTEC.

The ADCAM system integrates a personal computer with a multichannel analyzer (MCA), several computer-controlled instruments, and software to provide a workstation for performing high-quality measurements. The workstation uses a personal computer for data acquisition and data reduction for experimental results. The detector absorbs the energy from the incident gamma ray and produces a current pulse which is proportional to the absorbed energy. This pulse is integrated, converted to a voltage pulse, and shaped by the preamplifier. Additional amplification and pulse shaping is provided by the main amplifier (shaping amplifier). Output pulses from this amplifier go to the MCA. Functions of the MCA include:

1. Counting the number of pulses (counts) from the detector. The number of pulses (counts) are related to the number of gamma rays coming from the sample and to the disintegration rate (activity) of the source.

2. Measuring the amplitude of each pulse, which is proportional to the deposited gamma-ray energy. This process is referred to as pulse height analysis (PHA). Since the size of the pulse can be correlated with the gamma-ray energy, PHA can identify different radionuclides in a sample.

The printout from the ADCAM system includes the identified gamma-ray energy, the gross counts and net counts corresponding to the identified gamma-ray peak, live time, and centroid channel number.

2.2.2 Performance Tests of Measurement Systems

Performance characteristics of measurement systems include: energy resolution, peak shape, and relative detection efficiency. The energy resolution is determined by the full width at half maximum (FWHM) of a spectral peak at 1.33 MeV from a calibrated ^{60}Co source. At least 4000 counts in the peak channel are necessary. Detailed measurement procedures are provided in the users' manual. The measured resolution should be compared with the Quality Assurance Data Sheet in the manual to determine if there is a significant discrepancy.

The spectral peaks should be nearly symmetrical, approaching a Gaussian shape. The quality of the peak shape is determined at a specific height other than the half maximum. The full width at tenth maximum (FWTM) is measured, and the tenth-to-half ratio (FWTM/FWHM) is calculated. The ratio of FWTM/FWHM for a Gaussian peak is 1.823.

Detector efficiency is usually quoted by specifying the photopeak efficiency relative to that of a standard NaI(Tl) scintillation crystal. "A calibrated ^{60}Co point source is placed 25 cm from the center of the detector to determine the absolute efficiency of the germanium detector for 1.33 MeV photons. At least 20,000 counts should be accumulated in the 1.33 MeV peak."[7] The ratio of the absolute germanium detector efficiency to the efficiency of a 3 × 3 in. NaI scintillation detector at 25 cm (known to be 1.2E−3) is calculated. This ratio, expressed as a percentage, gives the relative efficiency of the detector ($R.E_f$):

$$R.E_f = \frac{(\text{peak area})/[(\text{activity}) \times (\text{live time})]}{1.2 \times 10^{-3}} \times 100 \quad (1)$$

where the peak area is the number of counts at the peak, the activity is in disintegrations per second, and the live time is the real time minus total system dead time in seconds.

2.2.3 Calibration of Detection System

It is necessary to relate the channel number of a photopeak to the energy of the gamma ray that produced it prior to calibrating the detector. The efficiency of the detector is calibrated with a National Institute of Standards and Technology (NIST) traceable source.

2.2.3.1 Two-Point Energy Calibration of the MCA

The process of determining the relationship between channel number and energy is called the MCA energy calibration. Over the energy range of most interest, the relationship between channel number and energy is close to a straight line. This relationship can be expressed as:

$$E_\gamma = mX + E_0 \quad , \quad (2)$$

where E_γ is gamma-ray energy (keV), X is the channel number of the photopeak centroid, m is slope (keV/channel), and E_0 is the intercept (keV). The slope and intercept are usually

determined by a linear least-square analysis, which is automatically calculated by the system. Quadratic fits are often used in research laboratories.

Two peaks are needed for the straight-line energy calibration. The radioisotope ^{154}Eu, with an energy range of 123.1–1274.4 keV, is used as the standard calibration source. The system is calibrated at a specified amplifier gain and the cursor reads in KeV.

2.2.3.2 Efficiency Calibration

It is customary to choose the Full Energy Peak Efficiency (E_P) as the detection system efficiency for a semiconductor detector. The E_P is defined as the probability that a gamma ray of energy E_r, emitted from the source, will appear in the photopeak of the observed pulse-height spectrum. This efficiency is a function of photon energy and is usually determined experimentally by using a selected NIST-traceable gamma ray standard source with precisely known gamma-ray emission rates. Factors affecting the detector efficiency are the detector itself, the detector-to-source geometry, the materials surrounding the detector, and the absorption in the source material.

Source-detector geometry is an important consideration in the efficiency calibration of detector systems and must be reproducible with good precision. Rate-dependent factors such as dead time and summation effects are also necessary to allow accurate efficiency determinations. The irradiated blood sample usually contains low-level activity; thus, the dead time and coincident summation effects can be neglected and the blood sample may be counted at the center of the end cap of the detector. Saline solutions were placed in a 20-mL scintillation glass vial for the experiments described in Sects. 2 and 3. The traceable calibration gamma-ray source was diluted and contained in a similar glass vial and counted on the top center of the detector, in order to keep the same source-detector geometry, absorption in the source material, and level of emission rate as the blood sample.

The gamma-ray reference standard used for this calibration consists of QCY.48 solution in 4 *M* HCL.[8] Eight mixed radionuclides in solution are listed in Table 1. A volume of 0.2 mL of QCY.48 was diluted by 20 mL of distilled water in a 20-mL glass vial. The emission rates from nuclides in the calibration source are also described in Table 1. The formula for calculating efficiencies is

$$E_{pi} = \frac{C_i}{T \times I_{pi} \times A_{oi} e^{-\lambda t}} \quad , \qquad (3)$$

where E_{pi} is the efficiency corresponding to each nuclide decay in the calibration source, C_i is the net counts under each peak, T is the live time (real time minus total system dead time), I_{pi} is the gamma-ray decay intensity, λ is the decay constant of each nuclide, and A_{oi} is the emission rate of each nuclide in the calibration source.

The efficiency curve as a function of gamma-ray energy is shown in Fig. 2. The lower the energy of the gamma ray, the more likely the photoelectric effect will occur, so the detector has higher efficiency at lower energy. The efficiency will drop off below 90 – 100 keV because the lower energy gamma rays tend to interact with the cryostat end cap or the detector's outer

Table 1. Efficiency calibration standard (liquid QCY.48)

Parent nuclide	Gamma-ray energy (MeV)	Gamma rays per seconds per gram of solution	Half-life	Efficiency
^{109}Cd	0.088	636	525 d	5.925E-2
^{57}Co	0.122	585	271 d	5.250E-2
^{139}Ce	0.166	725	137.6 d	4.610E-2
^{113}Sn	0.392	2144	115 d	1.895E-2
^{137}Cs	0.662	2486	30 years	9.667E-3
^{60}Co	1.173	3272	5.27 years	5.440E-3
^{60}Co	1.333	3276	5.27 years	4.918E-3
^{88}Y	1.836	6553	106.6 d	3.345E-3

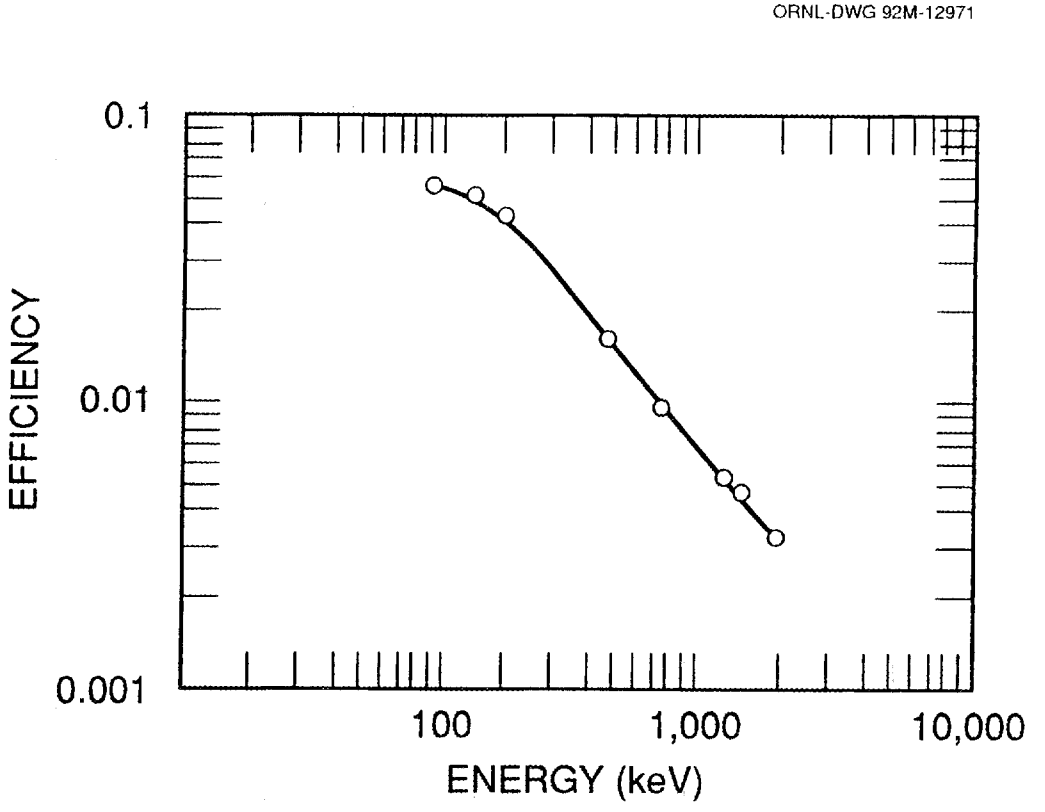

Fig. 2. Detection efficiency data for a 20-mL sample centered on the top surface of the GMX HPGe detector. The circles show measurement points for eight photon energies between 88 and 1836 keV, and the solid line shows the results of an empirical fit. QCY.48 solution was used as the reference standard source.

electrode before reaching the detector active volume. Counting efficiency for a specified peak can be determined from an efficiency curve or from the mathematical equation.

2.3 SALINE SAMPLE IRRADIATION AND COUNTING

The saline sample used in experiments consists of a 0.16-g quantity of salt and 20 mL of distilled water, since 100 mL of blood for a reference man contains 0.8 g of salt.[9] The neutron sources for irradiation are bare ^{252}Cf and D_2O-moderated ^{252}Cf. They are traceable to NIST and are located in the Radiation Calibration Facility (RADCAL) at Oak Ridge National Laboratory. The bare ^{252}Cf neutron spectrum, as shown in Fig. 3, is similar to an unshielded fission spectrum with an average energy of 2.5 MeV. The D_2O-moderated ^{252}Cf is a relatively soft spectrum and is illustrated in Fig. 4.

Irradiation positions of saline samples are shown in Fig. 5. Samples are placed on a standard 40 × 40 cm Plexiglas™ phantom. The distance from the source center (not the geometric center of the source capsule) to the center of the front face of the phantom varies from 10 to 25 cm for bare ^{252}Cf and 50 cm for D_2O-moderated ^{252}Cf. These irradiation situations are not the actual accident situations since a small bottle of saline on the phantom surface is used instead of a "reference man" phantom. However, the simulation will not affect reliability and accuracy as activity measurement procedures are established.

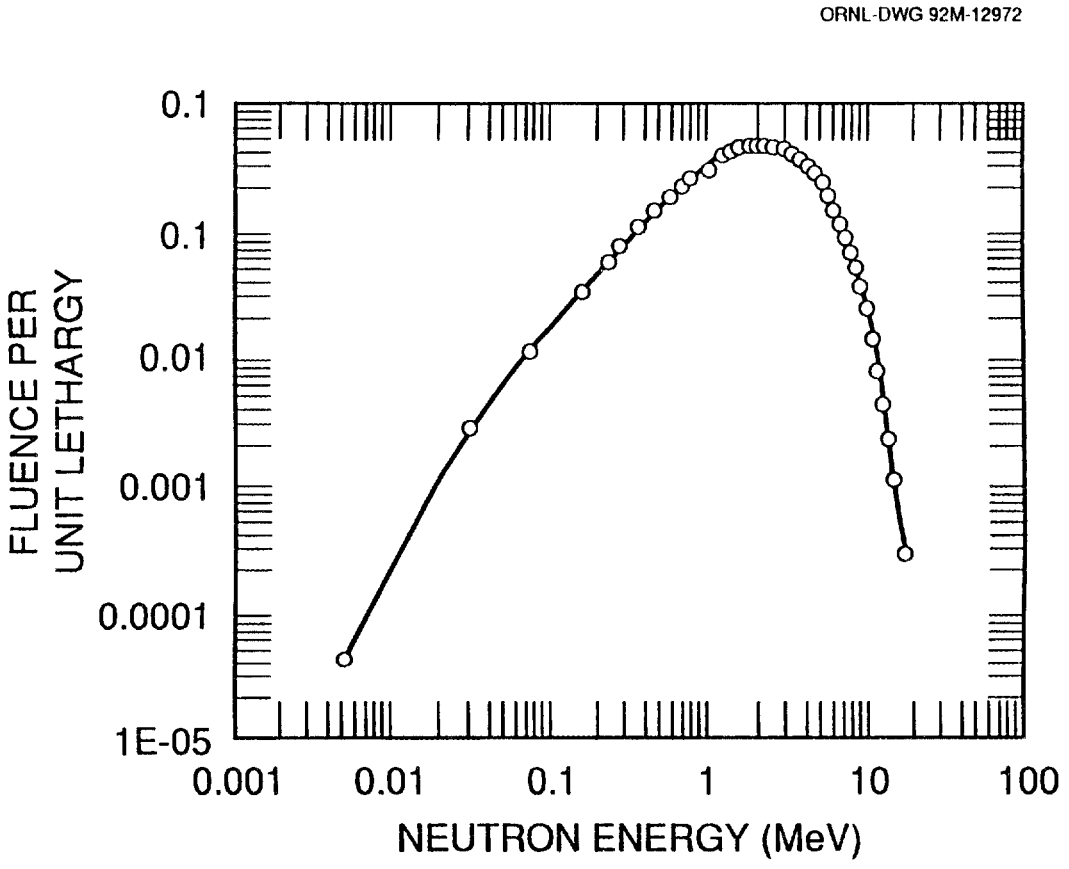

Fig. 3. Fluence spectrum of a bare ^{252}Cf source.

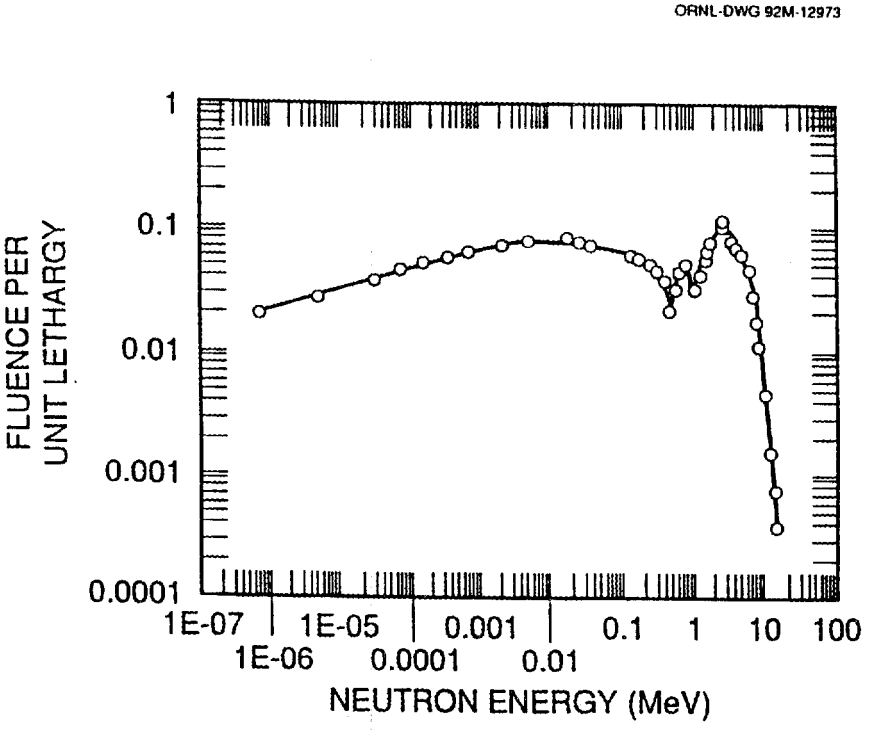

Fig. 4. Fluence spectrum of a D_2O-moderated ^{252}Cf source.

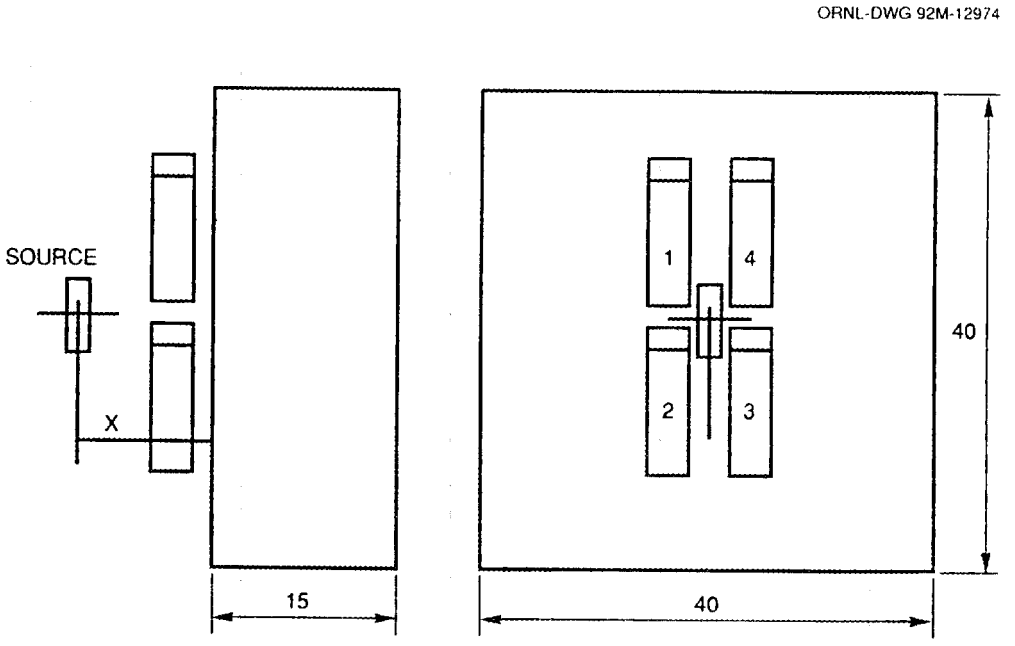

Fig. 5. A schematic showing irradiation positions of blood samples. Samples are placed on a standard 40 × 40 cm Plexiglas™ phantom. The distance from the source center to the center of the phantom surface varies from 10 to 25 cm for bare ^{252}Cf source and 50 cm for D_2O-moderated ^{252}Cf source.

The 1.368-MeV photopeak is used for counting ^{24}Na because it has a higher efficiency than the 2.75-MeV photopeak. Seventeen saline samples were irradiated with bare ^{252}Cf and D_2O–moderated ^{252}Cf at varying irradiation times and were counted at several different counting times.

2.4 BLOOD ^{24}Na CONCENTRATION CALCULATIONS

The specific ^{24}Na activity (A_{Na}) in blood is derived from the following equations:

$$A_1 = A_{Na} e^{-\lambda t_1} \quad , \tag{4}$$

$$A_2 = A_{Na} e^{-\lambda t_2} \quad , \tag{5}$$

and

$$A_1 - A_2 = \lambda C \quad , \tag{6}$$

where A_1 is the activity at the time counting starts, A_{Na} is the activity at the time of the end of irradiation by neutrons, t_1 is the elapsed time between the end of irradiation and the start of counting, A_2 is the activity at the time counting ends, and t_2 is the elapsed time between the end of irradiation and the end of counting. The difference between A_1 and A_2, $A_1 - A_2$, is the decayed activity during the counting period, where λ is the ^{24}Na decay constant, and C is the ^{24}Na count for the peak at 1.368 MeV corrected for background and counting efficiency. Thus, we obtain

$$A_{Na} = \frac{\lambda C}{e^{-\lambda t_1} - e^{-\lambda t_2}} \quad . \tag{7}$$

Two important factors affecting ^{24}Na concentration in blood are ^{24}Na biological decay and radioactive decay during an extended irradiation time. If the blood sample is collected several days after the accident, it is necessary to correct for the excretion of ^{24}Na from the body. The biological decay of sodium activity in the body can be represented by the sum of three exponential terms.[1] The fraction (R_t) of ^{24}Na retained in the body is given by

$$R_t = 0.487e^{-0.0815t} + 0.510e^{-0.0513t} + 0.0027e^{-0.0015t} \quad , \tag{8}$$

where t is the elapsed time from incident to collection of blood sample (days). The biological half-life is approximately 11 d, contrasting with the radioactive half-life of 14.7 h. Normally, the blood sample is taken within a few hours of the accident, and such a correction is not necessary. Biological decay is not considered because saline samples are used in the experiments.

Most criticality accidents happen in a very short time with an intensely high dose rate. However, the dose rate of neutron sources in RADCAL is lower. Irradiation of the sample from several hours to several days is necessary to yield a high dose. The short half-life of ^{24}Na will cause some loss of ^{24}Na activity in a longer irradiation time. The lost activity must be compensated by a decay correction factor. The factor is derived from the following equation:

$$\frac{dN(t)}{dt} = \varphi\sigma N_T(t) - \lambda N(t) , \qquad (9)$$

where $dN(t)/d(t)$ is the change rate of ^{24}Na produced at any irradiation time, $\varphi\sigma N_T(t)$ is the product rate of ^{24}Na at any irradiation time, $\lambda N(t)$ is the radioactive decay rate, and $N_T(t)$ is the concentration of ^{23}Na at any irradiation time, which is assumed to be constant. By solving Eq. (9), we obtain

$$A = \phi\sigma N_T(1-e^{-\lambda t}) , \qquad (10)$$

where A is the ^{24}Na activity at the end of irradiation time, excluding the decayed activity. If we exponentially expand $e^{-\lambda t}$ using Taylor series, then we obtain

$$A = \phi\sigma N_T\lambda t - \phi\sigma N_T\left[\frac{(\lambda t)^2}{2!} - \frac{(\lambda t)^3}{3!} + \frac{(\lambda t)^4}{4!} - \frac{(\lambda t)^5}{5!} - \ldots\right] \qquad (11)$$

and

$$A_{Na} = \phi\sigma N_T\lambda t , \qquad (12)$$

where A_{Na} is the total ^{24}Na activity produced at the end of irradiation time, including the decayed ^{24}Na activity. By comparing Eqs. (10) and (12), the decay correction factor (F_a) is found to be

$$F_a = \frac{\lambda t_a}{1-e^{-\lambda t_a}} , \qquad (13)$$

where t_a is the irradiation time.

Thus, the equation for calculating ^{24}Na activity in a blood sample is given by

$$A_{Na} = \frac{\lambda C_{net} F_a}{60 \times E_f I_r V R_t (e^{-\lambda t_1} - e^{-\lambda t_2})} \quad (Bq / mL) \quad , \qquad (14)$$

where

C_{net} = ^{24}Na net counts corrected for background (in cpm),

E_f = efficiency of detector for 1.368-MeV gamma rays,

I_r = fraction of gamma rays per disintegration (100%),

V = volume of blood sample (mL),

F_a = radioactive decay correction factor during the irradiation period, and

R_t = fraction of ^{24}Na retained in the blood at the time of blood sample collection.

Seventeen saline samples were irradiated by bare ^{252}Cf and D_2O-moderated ^{252}Cf. The highest neutron dose assigned to a saline sample was 6.42 Gy from bare ^{252}Cf at 10 cm. The lowest dose was 0.0185 Gy from D_2O-moderated ^{252}Cf. The measured data and calculated results are listed in Table 2.

The relatively consistent ratio between the neutron dose and measured ^{24}Na activity for the samples irradiated by the same neutron source indicates an acceptable repeatability of the ^{24}Na measurement process. Minor variations may be caused by: 1) variation of salt concentration in different saline samples, 2) uncertainty of measured dose, 3) changes in counting geometry, and 4) variation in counting statistics, which will be discussed in Sect. 2.5.

2.5 COUNTING STATISTICS AND ERROR ANALYSIS

Radioactive decay is a random process. Thus, any measurement based on observing the radiation emitted in nuclear decay is subject to a certain degree of statistical fluctuation. This fluctuation will cause an unavoidable uncertainty in a nuclear measurement. The fluctuation from a measurement can be analyzed using counting statistics analysis. Counting statistics analysis serves two purposes as used in nuclear measurements. It is used to determine if the fluctuation observed from a counting system is consistent with expected statistical fluctuation by counting the same sample repeatedly under the same counting conditions; this use is applicable to quality control procedures for counting equipment. Counting statistics analysis is also used to estimate how closely a single measurement corresponds to its "true" value when only one measurement of a particular quantity is available. Each blood sample measurement described in this report is a single measurement.

Table 2. Measured and calculated results for saline samples, including neutron dose, ^{24}Na activity, and ratios between dose and activity

Sample ID	Neutron source[a]	t_a (min)	t_i (min)	T (min)	C_{net}	F_a	A_{Na} (Bq/mL)	Dose (Gy)	D/A[b]
A	1	1256	364	90	704	1.56	5.99	1.90	3.16E-1
B	1	190	267	90	200	1.07	1.09	0.30	2.75E-1
C	1	277	458	90	153	1.11	1.13	0.38	3.35E-1
D	1	1574	588	90	781	1.73	7.73	2.52	3.89E-1
E	1	4223	743	90	1401	3.38	2.03	6.42	3.16E-1
F	1	2360	881	90	1234	2.17	1.27	3.90	3.05E-1
G	1	1153	524	90	1024	1.51	5.587	1.75	3.13E-1
H	1	235	426	90	326	1.09	1.195	0.36	3.02E-1
AA-1	1	1976	224	10	166	1.95	8.066	2.51	3.1E-1
AA-2	1	1976	236	30	540	1.95	8.88	2.51	2.84E-1
AA-3	1	1976	374	60	1022	1.95	8.473	2.51	2.97E-1
BB-1	2	1360	81	30	370	1.61	4.477	0.387	8.64E-2
BB-2	2	1360	121	60	774	1.61	4.884	0.387	7.91E-2
CC-1	2	1444	389	30	333	1.66	5.217	0.407	7.80E-2
CC-2	2	1444	424	60	657	1.66	5.365	0.407	7.59E-2
I[c]	2	3840	1560	30	2.57E4	3.12	8.658	0.679	7.84E-2
DD-1	3	538	218	120	1171	1.22	3.07	0.0187	6.07E-3
DD-2	3	538	1548	166	1714	1.22	3.326	0.0187	5.61E-3
FF-1	3	6216	111	10	121	4.83	38.48	0.216	5.6E-3
FF-2	3	6216	168	60	1932	4.83	37.74	0.216	5.7E-3
FF-3	3	6216	123	30	1032	4.83	38.48	0.216	5.6E-3
GG-1	3	7237	349	10	263	5.59	40.33	0.251	6.22E-3
GG-2	3	7237	1402	60	684	5.59	39.96	0.251	6.27E-3
HH-1[c]	3	5654	1518	60	601	4.41	30.22	0.188	6.21E-3
HH-2[c]	3	5654	1518	60	591	4.41	30.93	0.188	6.07E-3

[a]Neutron source 1 is bare ^{252}Cf at 10 cm. Neutron source 2 is bare ^{252}Cf at 25 cm. Neutron source 3 is D_2O-moderated ^{252}Cf at 50 cm.
[b]D/A is the ratio between neutron dose and ^{24}Na activity in 20 mL of saline sample (Gy/Bq/mL).
[c]Samples were counted at ORNL.

Since a nuclear transformation is a random, independent event, with a low probability for any one atom, the Poisson or Gaussian distribution (if the count of a sample is greater than 20) will be carried out to perform the counting statistics error analysis. We generally assume that a single count of a radioactive sample is an estimate for the mean of a Poisson or Gaussian distribution, and the square root of the count is the standard deviation. It is conventional to simply present the error of a single measurement as one standard deviation.

The estimated standard deviation of ^{24}Na activity (σ_A) is calculated from the standard deviation of the net counts (σ_{net}). The net counts (C_{net}) do not directly represent the number of counts from a specific source in a given counting time. The net count, C_{net}, is derived from gross counts (C_{B+C}) and background counts (C_B). Since we cannot associate the standard deviation with the square root of any quantity that is not a directly measured number of counts, the standard deviation of net counts, C_{net}, must be calculated according to the error propagation formula, Eqs. (15) and (16),

$$\mu = x + y + z \quad , \tag{15}$$

$$\sigma_\mu^2 = \left(\frac{\delta\mu}{\delta x}\right)^2\sigma_x^2+\left(\frac{\delta\mu}{\delta y}\right)^2\sigma_y^2+\left(\frac{\delta\mu}{\delta z}\right)^2\sigma_z^2 \quad , \tag{16}$$

where x, y, and z are directly measured counts, and μ is the quantity derived from these counts.

Thus, the standard deviation of C_{net} is given by

$$\sigma_{net} = \sqrt{C_{B+C}+C_B} \quad , \tag{17}$$

and

$$\sigma_A = \frac{\lambda F_a \sigma_{net}}{2.2 \times 10^6 E_f I_\gamma (e^{-\lambda t_1}-e^{-\lambda t_2})} \quad , \tag{18}$$

or in the form of specific activity,

$$\sigma_A = A_{Na}\sqrt{\frac{C_{B+C}+C_B}{C_{net}^2}} \quad Bq/mL \quad . \tag{19}$$

The statistical error is expressed as a percentage variation for convenience; that is, the standard deviation of the activity divided by the activity itself. It is expressed as

$$\% \sigma_A = 100 \frac{\sigma_A}{A_{Na}} \quad . \tag{20}$$

The calculated standard deviation and percentage variation of saline samples are listed in Table 3. The higher the accumulated net counts in samples, the lower the variation. The largest percentage variation is 11.5% for Sample C. It is caused by a very high background count and a low net count. The exact reasons that Sample C has a very high background count are unknown. Removing the lead shielding cover during counting or an unclear buffer may result in a high background count and, therefore, a large deviation.

2.6 SENSITIVITY OF THE MEASUREMENT PROCESS

The sensitivity of the measurement process is referred to as the required MDA in a sample at a given statistical confidence level. The lower the MDA, the higher the sensitivity of the measurement process. The MDA is expressed as

$$MDA = \frac{Constant \times Lower\ Limit\ of\ Detection}{Sample\ Size \times Efficiency \times Counting\ Time} \quad , \tag{21}$$

where the Lower Limit of Detection (*LLD*) of a detector is determined by the statistical maximum acceptable risk of making a Type I error, α (conclusion that sample counts exist when they do not exist) and a Type II error, β (conclusion that no counts exist when they do exist). The relationship between the LLD, Type I, and Type II errors is shown in Fig. 6.[10] The LLD at the 95% confidence level is approximately

$$LLD = (K_\alpha + K_\beta)\sqrt{2C_B} \quad , \tag{22}$$

where $K_\alpha = K_\beta = 1.645$. These values of K_α and K_β are based on a standard normal distribution and correspond to cases where the probability of making the Type I and Type II errors (α,β) is 5%. Equation (22) is suitable for the measurement situation where the background counts (C_B) in the region of interest are not accurately known beforehand. Therefore, the MDA for the blood sodium measurement system will be calculated using the following equation:

$$MDA = \frac{4.66\sqrt{C_B}}{60 \times E_f TV} \quad (Bq/mL) \, , \tag{23}$$

where E_f is the efficiency at 1.368 MeV energy, T is the counting time in minutes, and V is the volume of saline samples. The MDA is directly proportional to the standard deviation of background counts and inverse to counting time, efficiency of detector, and sample size. The four

Table 3. Results of counting error analysis

Sample ID	Gross counts	Background counts	Net counts	T (min)	A_{Na} (Bq/mL)	σ_A (Bq/mL)	σ_A / A_{Na} (%)
A	750	46	704	90	5.994	2.34E-1	4.0
B	244	44	200	90	1.092	7.84E-2	7.2
C	247	94	153	90	1.132	1.30E-1	11.5
D	848	67	781	90	7.733	2.94E-1	3.8
E	1469	68	1401	90	20.3	5.69E-1	2.8
F	1285	51	1234	90	12.72	3.77E-2	2.96
G	1080	56	1024	90	5.587	1.84E-1	3.29
H	373	47	326	90	1.195	7.51E-2	6.28
AA-1	177	11	166	10	8.066	6.54E-1	8.26
AA-2	552	13	540	30	8.88	3.88E-1	4.4
AA-3	1062	40	1022	60	8.473	2.71E-1	3.2
BB-1	392	22	370	30	4.477	2.46E-1	5.5
BB-2	801	27	774	60	4.81	1.78E-1	3.7
CC-1	355	22	333	30	5.217	3.02E-1	5.8
CC-2	684	27	657	60	5.365	2.18E-1	4.06
DD-1	1299	128	1171	120	3.074	9.88E-2	3.22
DD-2	691	67	624	166	3.323	1.46E-1	4.41
FF-1	387	37	350	60	38.48	2.26	5.88
FF-2	1068	36	1032	10	40.33	1.21	3.22
FF-3	1991	59	1932	30	39.96	8.99E-1	2.34
GG-1	287	24	263	10	30.22	2.70	6.7
GG-2	756	72	684	60	30.93	1.68	4.2

ORNL-DWG 92M-12989

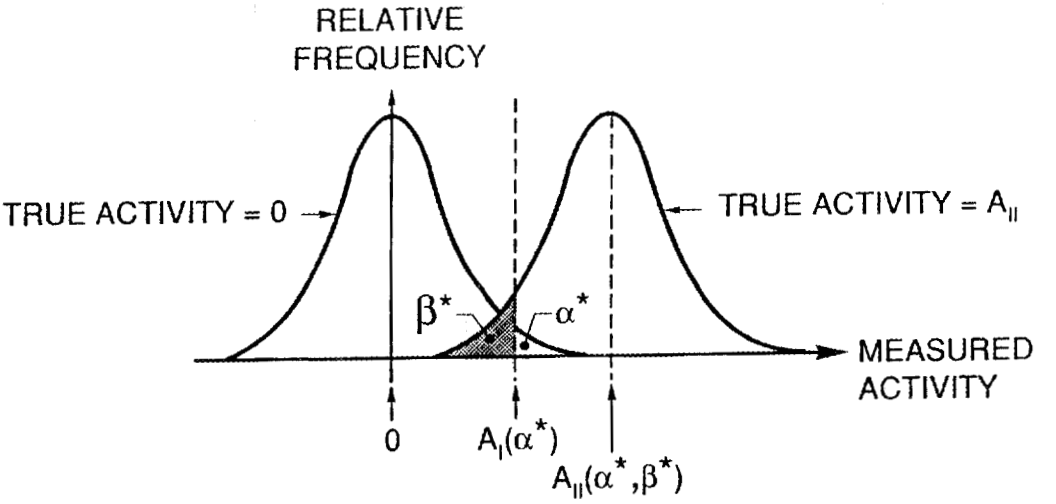

Fig. 6. Graphical illustration of Type I and Type II errors.

variables on the right-hand side of Eq. (23) are usually interrelated. The calculated MDA for saline samples counted at the University of Tennessee, Knoxville, are listed in Table 4.

The MDAs vary slightly for the same counting time as the background changes. The MDA is approximately 7.8E-2 Bq/mL for a 90-min count, 8.9E-2 Bq/mL for a 60-min count, 1.48E-1 Bq/mL for a 30-min count, and 5.18E-1 Bq/mL for a 10-min count for a system with an efficiency of 4.5E-3. Depending on the moderation of the neutron spectrum, 0.01-0.02 Gy of total neutron dose from the hardest spectrum can be detected for counting 30-60 min with a 95% confidence level. For soft spectra, the neutron dose less than 0.001 Gy can be readily detected with a 10-min count.

Table 4. Minimum detectable activity for saline samples counted at UT

Sample ID	Counting time (min)	MDA (Bq/mL)
A	90	7.289E-2
B	90	6.91E-2
C	90	1.043E-1
D	90	8.806E-2
E	90	8.88E-2
F	90	7.659E-2
G	90	7.807E-2
H	90	7.363E-2
AA-1	10	3.207E-1
AA-2	30	1.165E-1
AA-3	60	1.02E-1
BB-1	30	1.513E-1
BB-2	60	8.399E-2
CC-1	30	1.52E-1
CC-2	60	8.399E-2
DD-1	120	9.139E-2
DD-2	166	4.773E-2
FF-1	60	9.805E-2
FF-2	10	5.809E-1
FF-3	30	2.479E-1
GG-1	10	4.736E-1
GG-2	60	1.369E-1

3. DEVELOPMENT OF MEASUREMENT PROCEDURES FOR ^{32}P IN HAIR

3.1 INTRODUCTION

Measurement of fast neutron fluence is one of the most important components of an accident neutron dosimetry system. Most of the recoil dose in an actual accident is received from neutrons with energies greater than 100 keV, and the initial estimation of an accident neutron spectrum requires rapid assessment of neutron information. To date, the $^{32}S(n,p)^{32}P$ reaction in hair with a threshold neutron energy, 2.5 MeV, is the best choice for determining the fast neutron information using body activation.[1] Phosphorus-32 is a pure beta emitter with a maximum energy of 1.7 MeV and a 14.3-d half-life.

Human hair and fingernails possess sufficient sulfur for incident fast neutron fluence estimates. Only hair, especially on the head, is readily available in sufficient quantity to permit analysis after an accident. Sulfur is naturally present in human hair at a composition of 45 mg/g hair with little variation from individual to individual or with anatomical distribution.[11] By contrast, hair contains almost no phosphorus except that contributed by epidermal cell fragments and external contamination. The almost complete absence of natural phosphorus in hair permits its use as a biological sulfur threshold detector for determination of the incident dose of neutrons with energies in excess of 2.5 MeV.[11] Analysis of hair samples taken from the front, left, right, and back areas of the body and the head can also provide important information about the person's orientation at the time of the accident, based on the relative specific activity of each sample.

After the accident, if the individual has not been contaminated by fission products or fissile material, the ^{32}P activity can be counted directly on a beta detector. If the person has been contaminated very seriously, a more complicated chemical separation procedure may be required.[12] In most cases, the preferred technique for accuracy and simplicity is direct counting of hair. In the 1960s, scientists conducted several experiments on hair with direct counting using a low-background beta counter. The sensitivity of the process was 0.2 Gy (above 2.9 MeV) for a 1-g sample.[13] Since the priority for medical treatment after an accident is determined by the absorbed dose, a highly sensitive activity measurement process is required. In the past decade, the multichannel liquid scintillation spectrometer was developed with a low background and high efficiency. This development provides a possibility for improving the hair activity measurement process. Another advantage of liquid scintillation counting is that it can easily cut off the ^{32}P counts below a certain beta energy. Since most of the contaminating activity is of much lower energy than ^{32}P, the absence of some low energy activity can still provide an accurate preliminary estimate of ^{32}P activity without the chemical treatment when the sample is slightly contaminated.

The lost activity can be accounted for when calculating ^{32}P activity when necessary. The measurement system for ^{32}P activity in hair, hair sample preparation, activity counting process, calculation of ^{32}P activity, and MDA of hair measurements are discussed in Sect. 3.

3.2 MEASUREMENT SYSTEM FOR PHOSPHORUS IN HAIR

Liquid scintillation counting principles, components of the counting system, calibration and verification of performance tests of the counting system, and a counting efficiency determination for ^{32}P in hair are described in Sect. 3.2.

3.2.1 Liquid Scintillation Counting

A liquid scintillation sample usually consists of the radioactive material to be counted and the scintillation solution. The scintillation solution is also referred to as the cocktail. The cocktail is a mixture of a solvent and a solute, all contained in a sample vial. The main functions of the solvent are for dissolution of the sample and solute and absorption of the kinetic energy from beta particles. Ninety to 95% of the concentration in the cocktail is solvent. When a radioactive atom decays in the sample, several events occur. Some of the radiant energy released in the decay process is transferred to the solvent molecules which, in turn, transfer this energy to solute molecules. The solute molecules become excited by accepting this extra energy from the solvent. The excited molecules quickly return to the ground state, releasing the excess energy in the form of photons (see Fig. 7). Approximately 150 eV are required to produce one photon. "The intensity of photons in the scintillation is proportional to the initial energy of the beta particle. These photons escape from the vial and impinge on the face of the photomultiplier tube (PMT) and then cause the release of a photoelectron inside the tube. Each of these photoelectrons is then multiplied within the tube. This multiplication process results in the production of a measurable electrical signal which can be processed."[14]

Usually, there are two types of solutes in the cocktail. The primary solute absorbs energy from the solvent and emits photons with 3500- to 3700-Å wavelengths. However, the sensitive range of the PMT photocathode is 4200-4500 Å. The secondary solute (wavelength shifter) is needed to absorb the short-wavelength photons and then emit the long-wavelength photons for producing a greater response from the PMT.

"In terms of liquid scintillation counting, all radioactive decays are multiphoton events. The scintillation counter takes advantage of this fact and uses two PMTs to separate the real nuclear decay events from nondecay events. The energy of a nuclear decay event is dissipated in a period of time on the order of 5.0E-9 s. Thus, a beta decay having a multiplicity of photons will stimulate both PMTs at the same instant in time. The signal from each PMT is fed into a circuit which produces output only if the two signals occur together; that is, within the resolution time of the circuit, approximately 20.0E-9 s."[14] This is termed a coincidence circuit, as shown in Fig. 8, and the output of the circuit is a coincidence pulse.

The coincidence circuit prevents some single-photon events from passing on for analysis. These nonnuclear, single-photon events include electrical "dark noise" which originates from the photomultiplier tubes, inevitable background produced by environmental radiation, chemical reactions that generate chemiluminescence, and/or photoluminescence in the sample.

The so-called "internal liquid scintillation counting" (the radioactive material is in direct contact with the scintillation) and coincidence counting offers many unique measurement advantages, including homogeneous sample geometry, no absorption effects for beta radiation, and maximum radionuclide counting efficiency.

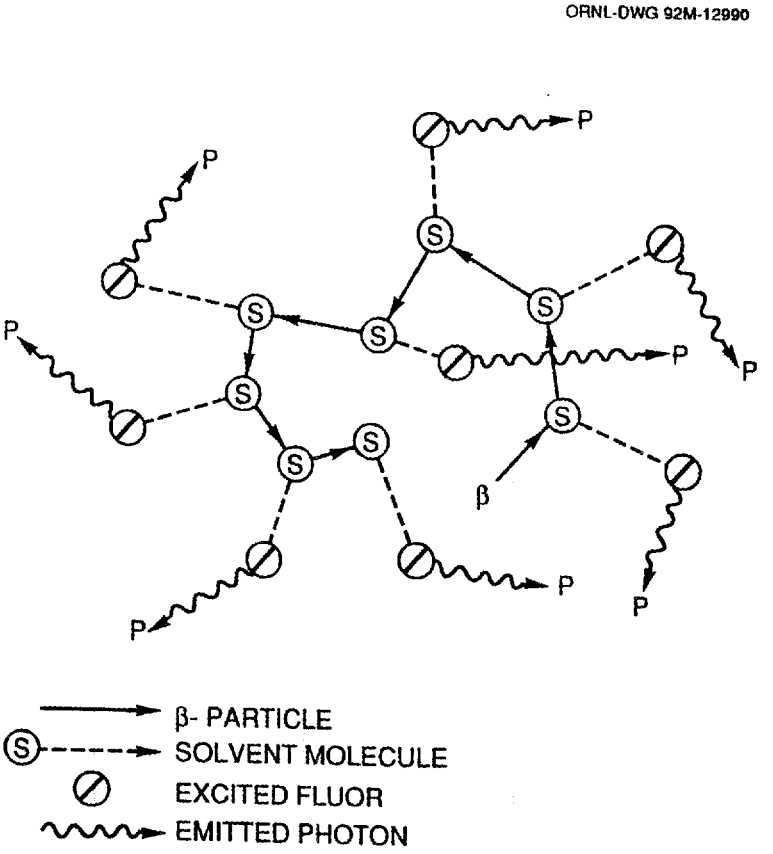

Fig. 7. Illustration of the collision process when a beta particle interacts with the liquid scintillation.

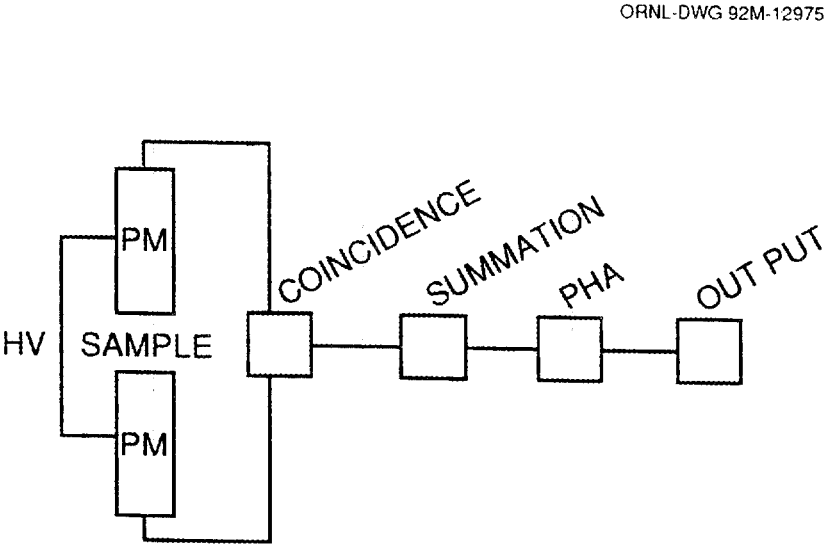

Fig. 8. A schematic of the liquid scintillation counting system.

3.2.2 Components of the Counting System

The Packard 2000 system used at the University of Tennessee, Knoxville, consists of the following major parts:

1. Scintillation detector.

2. Varisette™ sample changer which provides the means for sample movement to and from the detector.

3. Spectralyzer™ spectrum analyzer. The coincident summed pulses from the detector system are accumulated and analyzed in a spectrum analyzer circuit. The Spectralyzer™ spectrum analyzer also provides a method to determine the efficiency of the system. A spectral index of the sample (SIS) is calculated and related to the quenching level of the sample.

4. IBM-compatible PC which controls all instrument functions. Defining or editing a protocol program can simply be accomplished using the keyboard.

5. A printer.

3.2.3 Detector Performance Testing

The following performance verifications should be conducted daily:

1. carbon-14 efficiency check,

2. hydrogen-3 efficiency check, and

3. background check.

The performance verification specifications are as follows:

1. a minimum acceptable efficiency of 90% for unquenched ^{14}C,

2. a minimum acceptable efficiency of 58% for unquenched ^{3}H, and

3. a background of less than 30 cpm in the range of 0–19 keV.

3.3 PHOSPHORUS-32 COUNTING EFFICIENCY DETERMINATION

The factors affecting the liquid scintillation counting efficiency, interferences to the liquid scintillation process, and the efficiency determination for ^{32}P in hair are described in Sect. 3.3.

3.3.1 Quenching

In liquid scintillation counting, quenching and counting efficiency are closely related. There are essentially two types of quenching: chemical quenching and color quenching. Chemical

quenching interferes with the scintillation process by de-excitation of the solvent and causes energy losses in the beta energy transfer from solvent to solute before the beta energy is converted to photons.[15] Color quenching is the attenuation of light photons in the solution. Thus, it lessens the probability of transfer of photons to the cathode of the PMT.[15] Both chemical and color quenching cause energy loss in the liquid scintillation solution. As a result, the energy spectrum detected from the beta emitter shifts toward lower energies as illustrated by Fig. 9. Due to the change in energy distribution, it appears that the counting efficiency depends on the degree of quenching and, thus, on the nature of the sample, the scintillator used, and the sample preparation method.

The energy of beta particles plays an important role in determining the counting efficiency. The coincidence requirement that each PMT produces a response sets a limit of detection. The beta particle must have sufficient energy to produce at least two photons, and one must interact with each PMT. Inevitably, because the photons radiate in all directions, some will be lost. Thus, the probability of a photon entering each PMT decreases with decreasing beta particle energy.[16] High-energy beta particles produce excited and ionized solvent molecules which are relatively isolated from each other. The magnitude of each pulse produced is proportional to the energy deposited in the scintillator. Low-energy beta particles produce them in close space in regions of high-ionization density in which energy is dissipated in nonradiative transitions. This process is referred to as "ionization quenching" by Birks.[17] It will reduce the efficiency of the low-energy beta particle counting. Since ^{32}P has a very high maximum beta energy, the efficiency lost at lower energy is less than most of the other beta nuclides such as ^{14}C. This advantage can be used to trace ^{32}P counting efficiency by using ^{14}C quenched standards (see Sect. 3.3.3).

The application of high-resolution spectrum analysis of the Packard 2000 allows the calculation of two efficient and very accurate parameters to monitor quenching levels: the SIS and the Transformed Spectral Index of the Internal Standard Spectrum (tSIE).

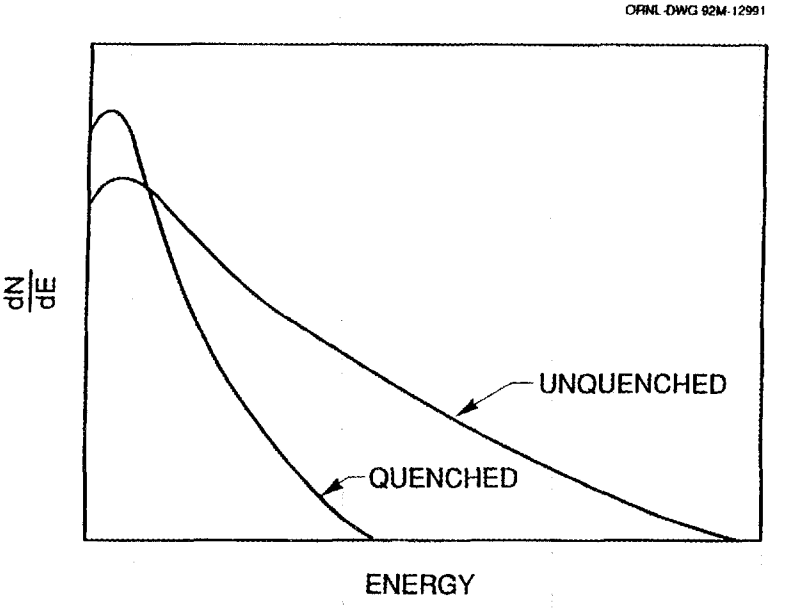

Fig. 9. Quenching effect of liquid scintillation counting. The beta energy spectrum shifts toward lower energies as a result of the quenching effect.

3.3.2 Counting Interference

The following interferences are common to the liquid scintillation process.

1. chemiluminescence,
2. photoluminescence,
3. static electricity,
4. heterogeneous samples,
5. background produced by environmental radiation, and
6. random electrical noise.

Chemiluminescence is the production of light as a result of a chemical reaction. This occurs typically in samples which contain peroxides or indicate an alkaline pH. A 30% hydrogen peroxide will be used in hair sample preparation. "Photoluminescence results from the activation of the cocktail and/or vial by ultraviolet light, such as sunlight or ultraviolet light sources used in the laboratory. Since a luminescence spectrum is quench-independent and is a single photon event, it is easy to distinguish from a beta energy spectrum using spectrum analysis."[15] The Packard 2000 counter can correct the counting results for luminescence influences.

Static electricity is another common source of counting interference, especially in dry weather. The buildup and subsequent discharge of static electricity on liquid scintillation vials is independent of quenching, and the pulse height is limited to 10–12 keV.

Heterogeneous effects are encountered for insoluble samples or for two-phase samples. This could occur when ashed hair samples are prepared using Triton if the solution in the vial is not homogeneous prior to counting (see Sect. 3.4.3). The counting efficiency of insoluble samples will be decreased and unstable. When two phases are present, each phase will have its own counting efficiency. The Packard 2000 counter warns the user when heterogeneous samples are encountered.

3.3.3. Tracing Counting Efficiency of ^{32}P in Hair

For the determination of ^{3}H and ^{14}C absolute activity, commercially manufactured quench standards are available. These standards can be used to generate quench curves, either manually or automatically, for the calculation of activity values of unknown samples of the same radionuclide. However, no commercial quench standards for ^{32}P are available since it has a relatively short radioactive half-life. The laboratory preparation of such quench standards is time-consuming and impractical in an emergency situation. A comparison of ^{14}C quenching with ^{32}P quenching will be used to estimate the quenched ^{32}P counting efficiency.

There are two methods, SIS and tSIE, for relating the efficiency and quenching levels in a Packard 2000. The Packard 2000 uses the distribution of the counts along the energy axis to monitor quench. By weighting each pulse by its energy, the mean pulse of the spectrum for any sample can be determined. This mean pulse, called SIS, is correlated with counting efficiency

or quenching. For an unquenched sample of any radionuclide, SIS value is close to its theoretical maximum energy.[15] The Packard 2000 also uses an external standard quench correction system, tSIE. This method is based on the fact that when both the sample vial and solution are irradiated by a gamma source, Compton electrons are produced within the sample. "The basic principle is that these Compton electrons behave as the beta particles emitted by the radioactive sample in solution and any quenching in the sample results in a proportional quenching of the Compton electrons. The number of Compton electrons produced is related to the strength of the gamma source which is adjusted to produce a statistically significant number within an additional period of counting time."[16] An important advantage of the tSIE method is its independence from sample activity. Most hair samples have a low count rate; thus, the tSIE is used to determine the quenching level index, tSIE. Typical tSIE quench curves for ^{14}C and ^{3}H are shown in Fig. 10 as a function of quenching level. The tSIE value for any unquenched radionuclide is 1000.

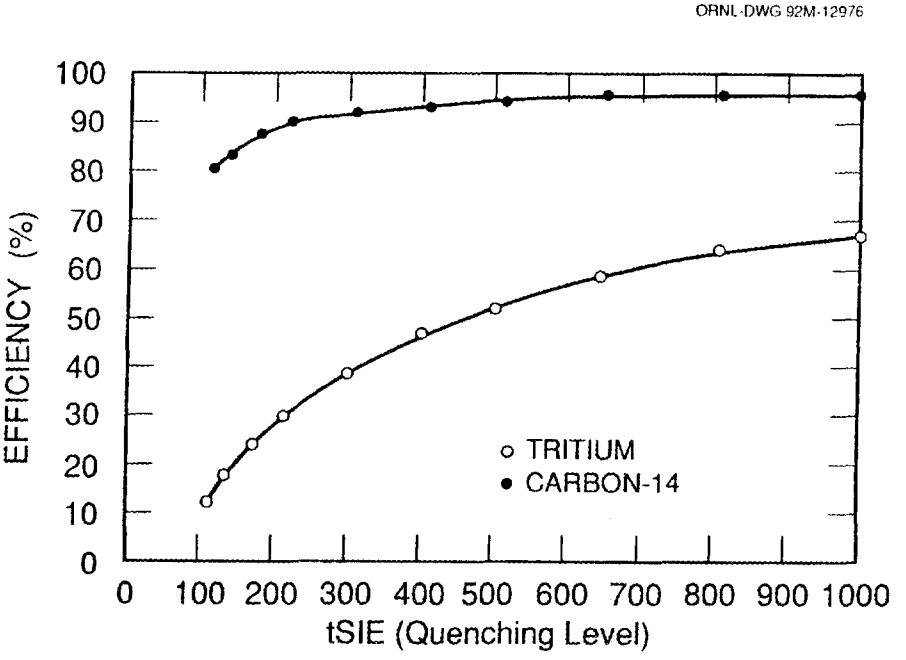

Fig. 10. Detection efficiency curves for liquid scintillation counting of ^{3}H and ^{14}C samples at different quenching levels.

As shown in Fig. 10, for the same tSIE values or same quenching levels, the efficiency of ^{14}C is much higher than ^{3}H since ^{14}C has much higher beta energy than ^{3}H. The maximum beta energy of ^{14}C is 156 keV. The maximum energy of ^{3}H is 18.6 keV. Above 300 tSIE, the efficiency for counting ^{14}C is almost constant and not affected much by the change of quenching level. The maximum efficiency for ^{14}C is 94%. Therefore, since the maximum beta energy of ^{32}P is 1700 keV, which is much higher than ^{14}C maximum energy, we can confidently assume that the counting efficiency of ^{32}P is constant within a wide range of quench levels and near its maximum efficiency. A 95% counting efficiency can be conservatively given to the activity measurement for ^{32}P in hair when the quenched ^{32}P standards are not available.

To verify this assumption, a series of experiments was conducted. The degree of quenching in the chemically prepared hair samples is determined by the amount of chemical-dissolving material and the hair weight handled by the solubilization method. In this case, the counting efficiency is affected by the chemical quenching, color quenching, and degree of solubilization of the sample. Differing amounts of hair and a ^{32}P isotope with equivalent activity were dissolved in eight similar glass vials, using differing amounts of chemical materials, and counted. The quenching level is increased as a function of the amount of hair dissolved and of the chemical materials as shown in Table 5. Significant quenching occurs when more than 0.5 g of hair is dissolved. The slight variation in ^{32}P count rates is probably caused by the errors in the ^{32}P dilution process since a very small amount of ^{32}P isotope was transferred with a digital pipe.

Table 5. Relationship between quenching and hair sample weight

Sample ID	Sample weight (g)	tSIE	cpm
1	0.0338	380	43170.4
2	0.0502	356	44544.9
3	0.0725	332	42273.9
4	0.0979	344	43243.9
5	0.1341	229	43726.4
6	0.2149	223	44470.9
7	0.3140	195	42870.9
8	0.5053	100	41908.4

3.4 HAIR SAMPLE PREPARATION

The efficient measurement of radioactivity in biological material by a liquid scintillation counter requires close contact between the sample and counting solution to reduce self-absorption. The hair samples should be pretreated before counting. Chemical dissolution and high-temperature ashing were evaluated to establish the relationship between quenching and sample weight analysis procedures.

3.4.1 Hair Washing

Silicon-31 is produced from oil, dust particles, and dry skin on the surface of the hair[13] and has a half-life of 2.6 h. The hair should be washed if the sample is counted shortly after the accident, even if uncontaminated by fission products.

3.4.2 Chemical Dissolution of Hair

Methods used for producing homogeneous counting solutions from hair by chemical dissolution should be evaluated by:

1. ease of sample preparation;
2. maximum or optimal hair weight and volume handled by the solubilization method;
3. maximum efficiency related to hair weight; and
4. chemiluminescence.

The chemical solutions used are SX-10 tissue solubilizer, 30% hydrogen peroxide, and dithiothreitol (DTT). Each solution is prepared by the Fisher Scientific Corporation. Descriptions of each material are listed in Table 6. A series of experiments were conducted to obtain optimal amounts of the hair and chemical materials, along with detailed analysis procedures. Based on the experiments, it is concluded that 1 g of hair requires 12000–14000 μL of tissue solubilizer, 6000–7000 μL of hydrogen peroxide, and 0.12 g DTT.

Heating about 3–4 h at 50–60°C is also needed. The preferred, optimal order for adding chemical materials is hydrogen peroxide, tissue solubilizer, and DTT. The maximum amount of hair solubilized without severe chemical quenching and completely solubilized within 4 h is 0.3 g.

3.4.3 Ashing of Hair

Counting solutions may be prepared using ashed hair. A muffle furnace and crucibles are used in the ashing process. The experiments are conducted at temperatures ranging from 600–1000°C. Excessive amounts of char are developed below 700°C, and much of the hair is volatilized at 1000°C. The residual ash associated with the experiments performed at a temperature of approximately 800°C indicates that no char was produced and that essentially all of the ash remained in the crucibles. One gram of hair reduces to 0.008 g after ashing. Care must be taken in transferring the ashed hair to the liquid scintillation vial to assure that little

Table 6. Description of chemical materials used

Chemical materials	Description
Hydrogen peroxide (30%)	Acid solution helps tissue solubilizer to dissolve hair sample completely.
ScintiGest® tissue solubilizer	Ready-to-use 0.6*N* solution specifically formulated for rapid solubilization of tissue homogenates. Usually yields clear solution, rather than viscous, cloudy gels produced by other types of solubilizers.
Dithiothreitol (DTT)	Six grades of agarose and the highest grades of acrylamide, bisacrylamide and associated reagents are available for separation of proteins and nucleic acids by electrophoresis.

ashed hair is lost in the process. The loss of the ashed hair will remarkably affect the calculation of specific ^{32}P activity when the sample contains a small amount of hair. The ashed hair remains in a fine powder. Triton-100 is used for suspending the powders in the counting solution.

Based upon a comparison of the above hair preparation methods, chemical dissolving is recommended when the hair sample weighs below 0.3 g since the chemical quenching is relatively small. If a large hair sample is available, ashing hair is recommended due to less quenching. The consistency of ashing depends on the degree of suspension and careful operation.

The procedures for preparing background samples are the same as for preparation of hair samples. A "blank" background sample should simulate as closely as possible the chemical composition and physical form of an irradiated hair sample solution being measured. The "blank" hair can be obtained from an unirradiated individual.

3.5 HAIR SAMPLE COUNTING AND ^{32}P ACTIVITY CALCULATION

A series of hair samples was irradiated by a bare ^{252}Cf neutron source. The counting window (counting energy range) was set at 5-1700 keV. The counts below 5 keV were cut off due to unstable data. This was caused by some random "noise pulses" from the PMT, surrounding background, and unknown effects from chemical reactions. The printouts from the counting system include the count rate of sample and background count rate in the region of interest, counting time, quenching indicator (SIS, tSIE), and chemical luminescence indicator. Using the measured count rate, the ^{32}P activity is calculated by

$$A = \frac{C}{60 \times e^{-\lambda t} E_f m} \quad (Bq/g) \quad , \tag{24}$$

where

A = ^{32}P activity induced in hair (dpm/g),
C = cpm associated with the specified window setting,
λ = ^{32}P decay constant,
t = elapsed time from the end of the accident until the start of counting,
E_f = counting efficiency for ^{32}P, and
m = the amount of hair (g).

One standard deviation of calculated ^{32}P activity is given by

$$\sigma_A = A\sqrt{\frac{G_c + B_c}{C^2 \times T}} \quad , \tag{25}$$

where

G_c = gross cpm associated with the specified window setting,
B_c = background cpm associated with the specified window setting,
σ_A = one standard deviation of A, and
T = counting time, which is the same for sample and background counting (min).

The measured and calculated results are listed in Table 7. The highest neutron dose used was 5.41 Gy, and the lowest was 0.66 Gy. The largest sample contains about 1.0 g of hair. The smallest sample has about 0.16 g of hair. The ratios between specific activity of ^{32}P and dose vary slightly between 1.16 Bq/g per Gy and 1.44 Bq/g per Gy except samples LA1-A, 4-C, and 8-A. The variation corresponds to the repeatability of the measurement process. LA1-A and 8-A are small ashed samples and 4-C is a large chemically dissolved sample. They have relatively lower specific activities compared with other samples. This fact further confirms the conclusions in Sect. 3.4 that small ashed samples (below 0.3 g) and large chemically dissolved samples (above 0.5 g) will cause an activity loss if the operation process is not performed very carefully. Some inconsistent results for the same samples counted twice, such as LA2-A, are caused by the heterogeneous ashed sample solution. The ashed solution should be shaken before each counting since the Triton material in the solution can only be effective for 1-2 h each time.

The larger statistical counting error is associated with low count samples or small samples. According to Eq. (25), counting error can be reduced by increasing counting time.

3.6 SENSITIVITY OF MEASUREMENT SYSTEM

According to the theory in Sect. 2.6, the LLD for counting ^{32}P in hair will be

$$LLD = 4.66\sqrt{B_c T} \quad , \tag{26}$$

where B_C is the background count rate and T is the counting time in minutes.

The MDA is in the form of

$$MDA = \frac{4.66\sqrt{B_c}}{60 \times E_f \sqrt{Tm}} \quad Bq/g \quad , \tag{27}$$

where the MDA is proportional to the square root of the background count rate and inverse to the sample weight and square root of the counting time. To investigate the relationship among the background count rate, counting time and sample weight, a series of experiments using "blank" hair samples was conducted.

Table 7. Measured and calculated results for hair samples irradiated by different neutron doses

Sample ID	Sample weight (g)	Elapsed time[a] (h)	Counting time (min)	Net cpm	Specific activity[b] (Bq/g)	Total dose (Gy)	Activity-to-dose[c]	Standard deviation[d] ($\times 10^{-1}$)	σ_A/A (%)
11-C[e]	0.1746	88.32	20	14.2	1.72	1.34	1.283	2.75	15.6
33-C	0.166	126.1	40	28.65	3.926	3.39	1.161	2.279	5.789
55-C	0.1768	126.45	40	53.5	6.91	5.41	1.867	2.371	3.34
2-A[f]	0.5344	65.82	60	34.48	1.293	1.02	1.268	0.543	4.2
2-A	0.5344	73.02	30	33.47	1.275	1.02	1.250	0.793	5.79
4-C	0.5343	93.45	60	26.83	1.064	1.02	1.043	0.644	6.7
6-C	0.1619	169.1	60	10.95	1.467	1.02	1.438	2.101	13.91
8-A	0.1618	117.5	60	7.27	0.999	1.02	0.979	1.824	18
10-A	1.0563	77.133	30	55.53	1.214	1.02	1.190	0.518	4.2
10-A	1.0563	78.283	30	56.34	1.195	1.02	1.171	0.496	4.14
LA1-A	0.2135	132.03	60	6.55	7.1E-1	0.66	1.076	1.42	20.4
L1-C	0.2142	133.03	60	8.6	9.28E-1	0.66	1.407	1.78	19
LA2-A	0.5192	131.03	60	19.28	8.58E-1	0.66	1.300	0.633	7.47
LA2-A	0.5192	150.4	60	16.4	7.59E-1	0.66	1.149	0.651	8.6
AN1-A	0.5	161.67	40	17.2	8.44E-1	0.66	1.278	0.825	9.8

[a]Elapsed time after irradiation and before counting starts.

[b]Specific activity of ^{32}P in hair (Bq/g).

[c]Ratio of ^{32}P specific activity to measured total neutron dose (Bq/Gy).

[d]One standard deviation of A in hair (Bq/g).

[e]The -C suffix indicates that the sample is chemically dissolved.

[f]The -A suffix indicates that the sample is ashed.

Table 8 lists the experimental results from chemically dissolved "blank" hair samples. The background count rate does not change significantly with different counting times, but it increases as the sample weight increases. The averaged background count rate for chemically dissolved hair samples of about 0.16 g is 68 cpm; for samples of 0.2 g, 76.3 cpm; and for samples of 0.5 g, 87 cpm.

Table 9 lists the background count rate from ashed "blank" hair samples. The measured background count rates are almost constant regardless of the counting time and sample weight. The averaged background count rate is 50.3 cpm. This value is near the "blank" cocktail count rate, which is about 45 cpm in the window (5–1700 keV). The background count rate for the counter itself is 36 cpm in the same window.

The following conclusions are based on a comparison of results in Tables 8 and 9:

1. The background count rate of chemically dissolved hair samples increases as the weight of the hair in the sample increases.

2. The background count rate of ashed samples is almost constant and similar to the count rate of the cocktail solution.

3. The background count rate of chemically dissolved samples is higher than ashed samples.

4. The background count rates for both methods do not change significantly with different counting times.

The calculated MDAs based on the above conclusions are listed in Table 10. The lowest MDA is 0.0747 Bq/g of hair, derived from 1.0 g of ashed sample counted for 60 min. If we take the bare ^{252}Cf spectrum as a reference spectrum, about 0.06–0.07 Gy of total neutron dose can be measured from a 1-g hair sample with a 95% confidence level.

Table 8. Background count rate in window (5-1700 keV) from chemically dissolved "blank" hair samples

Sample weight (g)	Counting time (min)	Background (cpm)
0.1618	30	70.67
0.161	30	67.63
0.1605	60	65.75
0.2034	60	77.88
0.2021	60	75.38
0.2002	60	74.83
0.2056	30	77.08
0.5023	30	84.43
0.5054	60	85.45
0.51	30	89.13
0.5055	30	89.1

Table 9. Background count rate in window (5-1700 keV) from ashed "blank" hair samples

Sample weight (g)	Counting time (min)	Background (cpm)
0.1620	30	49.2
0.1615	60	49.3
0.22	60	52.78
0.2015	30	50.75
0.2022	60	51.02
0.5011	30	51.2
0.5111	60	49.27
0.5023	60	48.05
1.05	30	50.23
1.08	60	53.03

Table 10. Minimum detectable activity for counting ^{32}P in hair

Sample preparation	Sample weight (g)	Background count rate	Counting time (min)	LLD (counts)	MDA (Bq/g)
Chemical dissolution	0.16	68	30	210	0.7659
			60	297	0.5402
Ashing	0.16	50.3	30	181	0.6586
			60	256	0.4662
Chemical dissolution	0.2	76.3	30	222	0.6475
			60	315	0.4588
Ashing	0.2	50.3	30	181	0.5291
			60	256	0.3737
Chemical dissolution	0.5	87	30	238	0.2782
			60	336	0.1961
Ashing	0.5	50.3	30	181	0.2116
			60	256	0.1495
Ashing	1.0	50.3	30	181	0.1055
			60	256	0.0747

4. DEVELOPMENT OF AN ACCIDENT NEUTRON DOSE ASSESSMENT SYSTEM

4.1 INTRODUCTION

The production of ^{24}Na in the blood by neutrons is a function of total neutron dose, the accident neutron spectrum, the individual body size and body weight, the specific ^{24}Na concentration in an individual's blood, and the person's orientation during an accident. When an accident occurs, such detailed and accurate information is difficult to obtain within a few hours after the accident. However, a rapid accident neutron dosimetry system for initial dose assessment is necessary for doctors to treat the victims as soon as possible.

The most important and difficult step in the initial dose assessment is to determine the accident neutron spectrum within a few hours after the accident. Area dosimeter stations and computerized calculations can be used to obtain spectral information. However, they do not satisfy the limited time requirement.[1]

Griffith[4] and database files from ORNL[18] contain a large number of spectra for fission neutrons which have been transmitted through different thicknesses of various materials, as calculated by a Monte Carlo method.[4] These encompass the most likely neutron spectra encountered in nuclear accidents. These data provide a basis for a methodology to quickly approximate the actual spectrum in a criticality accident from sets of spectra after accidents.

Section 4 describes the development of an accident neutron dose assessment system using these neutron spectra and measured blood activity, the special functions of hair activation in accident neutron dosimetry, and quantities affecting the accuracy of the derived neutron dose.

4.2 DISCUSSION OF NEUTRON SPECTRA

One hundred seventeen different neutron spectra were supplied by ORNL in May 1991 in the form of database files.[4,18] Ninety-eight of them can be readily transferred from the database files to ASCII files.

4.2.1 Spectrum Description

In a nuclear accident, the geometry and material composition of the critical assembly and its environment can be very complex. Two approximations were assumed in the use of the 98 neutron spectra:[4]

1. The actual spectrum corresponds directly to that from the critical assembly or to one filtered by various materials. Multiple scattering from the room or from objects surrounding the individual is not considered.

2. The composition and thickness of the shielding material are much more important in determining the shape of the leakage spectrum than geometry of the critical assembly.[19]

Ninety-eight neutron spectra are grouped according to shielding configurations as listed in Table 11. Each group includes different radii of shielding and shielding materials.

4.2.2 Plots of Representative Spectra

All spectra are presented in the form of fluence per unit lethargy (per unit logarithmic energy) versus neutron energy in MeV. "The lethargy unit is preferred since neutron spectra, when plotted as fluence per unit energy, often display a steep negative slope at lower energies due to a roughly inverse-energy type of dependence and require many decades on the fluence axis for complete presentation. The lethargy unit essentially weights the fluence by the corresponding neutron energy, so the negative slope is changed to an approximately horizontal line which is simple to present graphically."[4]

All 98 spectra must be interpolated with similar energy boundaries because each spectrum has unique energy groups and energy boundaries. The integrating energy boundaries are 620 groups ranging from 10E−10 MeV to 18 MeV. A linear interpolation is used. Both original and interpolated uncollided fission spectra are shown in Figs. 11 and 12. The shape and magnitude of each plot is identical, thus verifying the interpolation.

4.3 NEUTRON DOSIMETRY USING BLOOD

A collection of 98 neutron spectra is utilized to develop a method for estimating neutron dose by the induced ^{24}Na activity in blood without the difficulty of an exact spectrum measurement and calculation. The intention is to convert the blood activity-to-fluence relation into an activity-to-dose relation by means of the known fluence-to-dose conversion factors. Thus, the neutron dose can be directly related to the blood activity based on information on the 98 neutron spectra.

4.3.1 Blood Activity-to-Fluence

Many calculations and experiments have been conducted to determine the relationship between the incident neutron fluence and the induced specific activity of ^{24}Na in the blood. An intermediate step in the relation between fluence and the specific activity of ^{24}Na is the capture probability,[20-21] which is the fraction of neutrons striking a phantom that is captured at thermal energy.

4.3.1.1 Capture Probability

"The human body is several mean free paths thick for fast neutrons. Thus, the probability that a fast neutron will be captured as a thermal neutron is not very sensitive to its initial energy."[20] Table 12 lists the calculated capture probabilities as a function of incident neutron energy for a BOMAB phantom.[1] The BOMAB phantom is a set of 10 NaCl solution-filled polyethylene bottles. Some of the bottles are elliptical and some are cylindrical. The shape and size of the BOMAB phantom will be used as a reference man in our calculations.

Table 11. Spectra description

1. Spectra from selected critical assemblies

   Uncollided fission spectrum
   Unshielded HPRR
   Concrete-shielded HPRR at 3 m
   Plexiglas™-shielded HPRR
   Steel-shielded HPRR at 3 m

2. Spectra from critical solutions

   Fissile H_2O solution
   Fissile D_2O solution

3. Spectra of fission neutrons through shielding

   Fission neutrons through H_2O
   Fission neutrons through D_2O
   Fission neutrons through graphite
   Fission neutrons through polyethylene
   Fission neutrons through 1% borated polyethylene
   Fission neutrons through beryllium
   Fission neutrons through aluminum
   Fission neutrons through concrete
   Fission neutrons through concrete + 10% iron
   Fission neutrons through concrete + 50% iron
   Fission neutrons through iron
   Fission neutrons through copper
   Fission neutrons through lead
   Fission neutrons through uranium-238

4. Spectra of H_2O-moderated fission neutrons through shielding

   H_2O-moderated fission neutrons through beryllium
   H_2O-moderated fission neutrons through aluminum
   H_2O-moderated fission neutrons through concrete
   H_2O-moderated fission neutrons through iron
   H_2O-moderated fission neutrons through copper
   H_2O-moderated fission neutrons through lead

5. Selected spectra

   Bare ^{252}Cf
   D_2O-moderated ^{252}Cf

ORNL-DWG 92M-12977

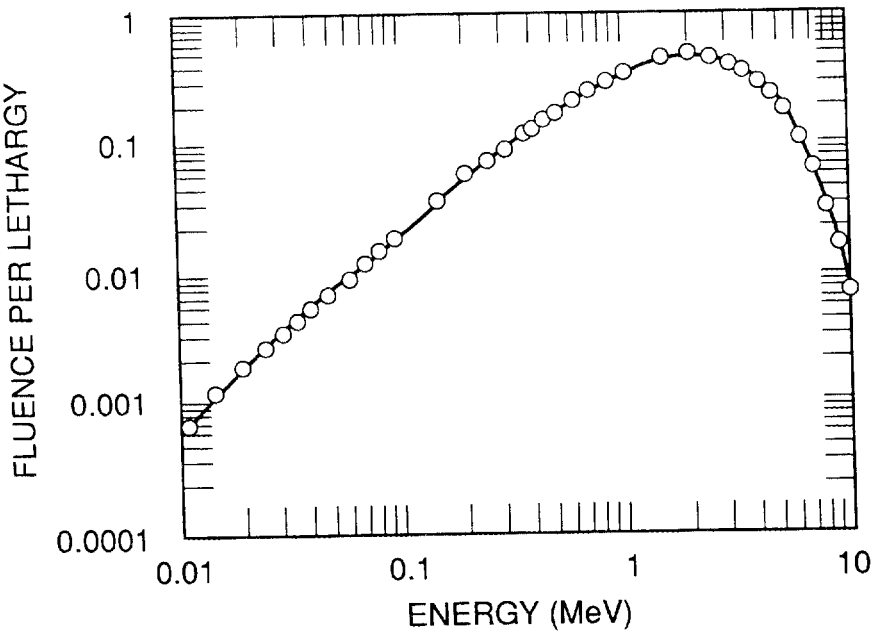

Fig. 11. Uncollided fission spectrum from IAEA Technical Report Series No. 318.

ORNL-DWG 92M-12978

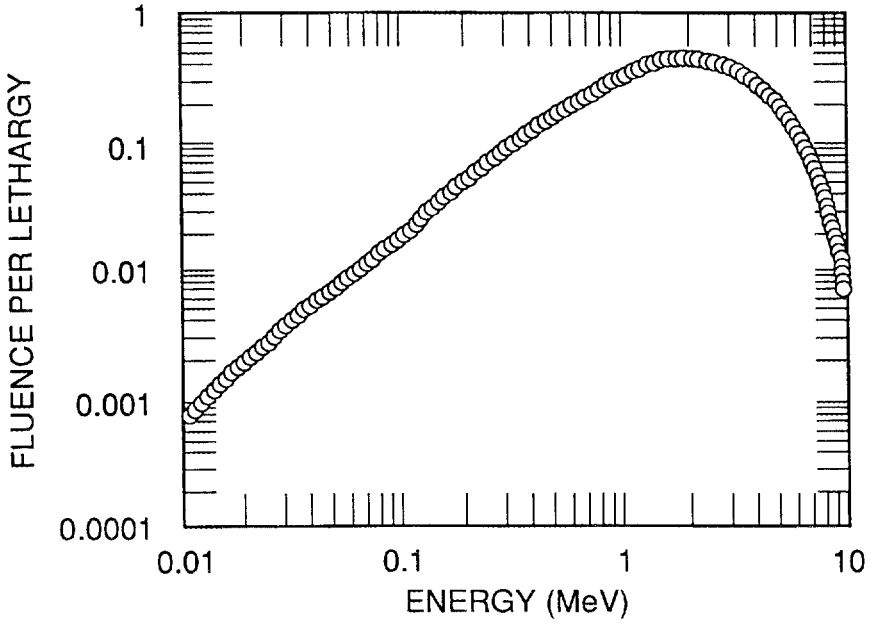

Fig. 12. Uncollided fission spectrum interpolated with selected energy boundaries.

Table 12. Capture probabilities for a BOMAB phantom

Neutron energy (MeV)	Capture probability	Neutron energy (MeV)	Capture probability
2.5E-8	0.186	1.0E+0	0.244
1.0E-6	0.301	1.2E+0	0.270
1.0E-5	0.338	1.4E+0	0.266
1.0E-4	0.335	1.8E+0	0.250
1.0E-3	0.313	2.0E+0	0.242
1.0E-2	0.296	2.4E+0	0.230
1.0E-1	0.292	3.0E+0	0.210
2.0E-1	0.293	3.4E+0	0.200
3.0E-1	0.294	4.0E+0	0.184
3.5E-1	0.290	4.5E+0	0.178
4.5E-1	0.251	6.0E+0	0.147
5.0E-1	0.303	10.0	0.140
6.0E-1	0.302	14.0	0.127
8.0E-1	0.288		

The moderation of the body to the incident neutrons is so strong that the interaction of $^{23}Na(n,\gamma)^{24}Na$ is mainly determined by the body capture probability, not the absorption cross-section of ^{23}Na. This is well illustrated by Figs. 13 and 14.

4.3.1.2 Relation Between Fluence and ^{23}Na Activation

When an incident beam of neutrons strikes perpendicularly (normally) to the axis of the phantom, the number of neutrons in the energy interval, dE, striking the phantom is $S\phi(E)dE$, where S is the projected area of the phantom to the beam. Of the total number of neutrons striking the phantom, a fraction $\xi(E)$ (capture probability) will be captured in the phantom, and the fraction of these which will undergo reaction of $^{23}Na(n,\gamma)^{24}Na$ is Σ_{Na}/Σ_t, where Σ_{Na} is the macroscopic absorption cross-section of ^{23}Na in tissue and blood, and Σ_t is the total absorption cross-section in the body.[20] Thus, the total number of ^{24}Na atoms produced in the phantom is

$$\frac{\Sigma_{Na}}{\Sigma_t}\int_0^\infty \xi(E)\, S\phi(E)\, dE \quad . \tag{28}$$

If the volume of the phantom is V and the ^{24}Na decay constant is λ, the specific activity of ^{24}Na per unit volume induced in the phantom is

$$A = \lambda\left(\frac{S}{V}\right)\left(\frac{\Sigma_{Na}}{\Sigma_t}\right)\int_0^\infty \xi(E)\,\phi(E)\, dE \quad Bq/mL \quad . \tag{29}$$

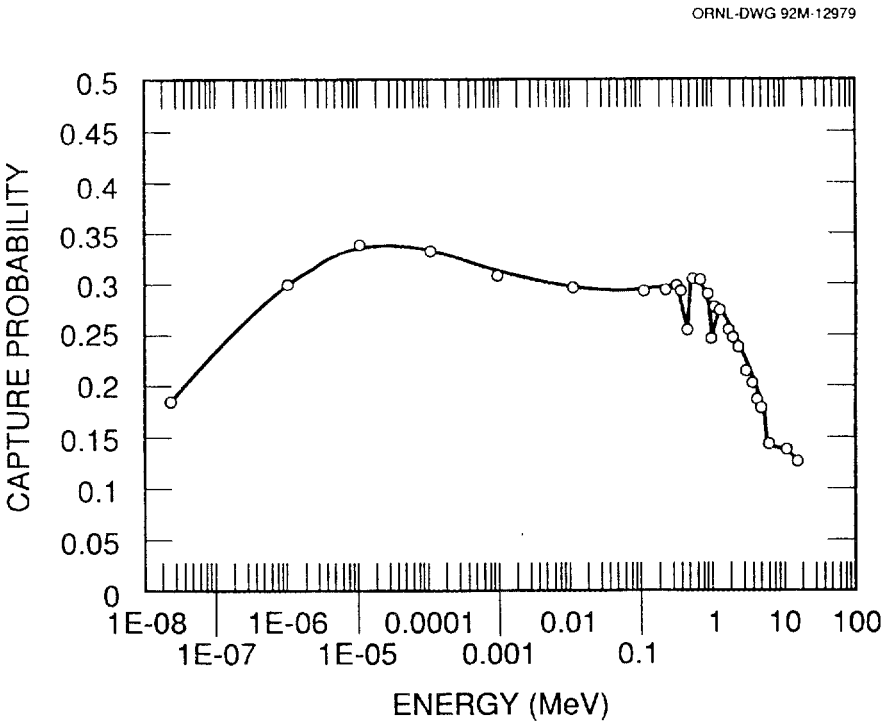

Fig. 13. Neutron capture probability for neutrons incident on the front body surface of the BOMAB phantom from calculations of Cross (1981).

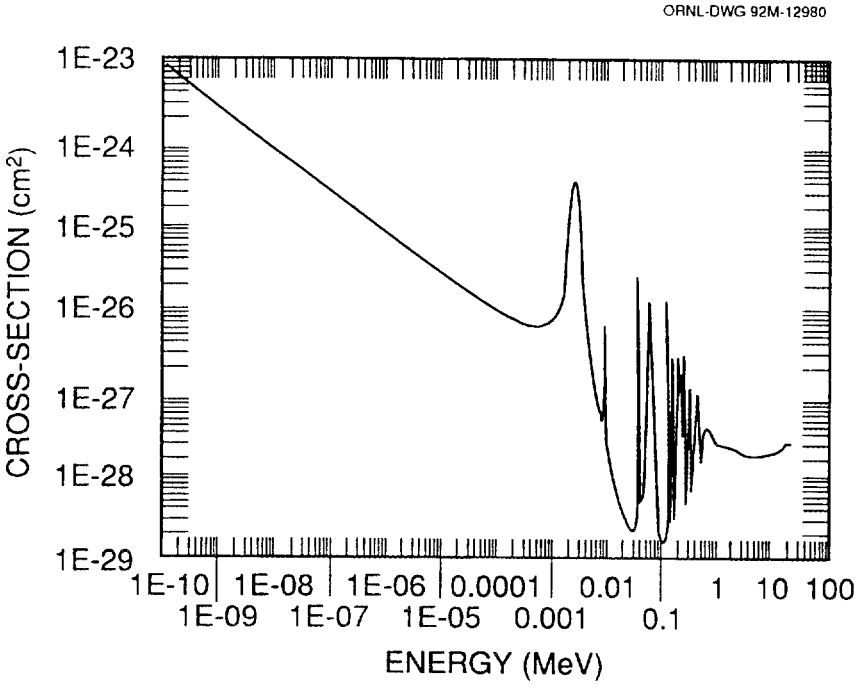

Fig. 14. Illustration of the cross section of the $^{23}Na(n,\gamma)^{24}Na$ reaction as a function of neutron energy (Garber and Kinsey, 1976).

This equation was first given by Hurst[20] and is used widely in the calculation of ^{24}Na activation. Since the ratio of the concentration of ^{24}Na and ^{23}Na ($^{24}Na/^{23}Na$) in circulated blood is equal to the ratio in the whole body,[22] we can conclude that the specific activity of ^{24}Na per unit volume of whole body is the same as the specific activity of ^{24}Na per unit volume of the blood.

The thermal spectrum-averaged macroscopic cross-section of ^{23}Na in Eq. (29) is given by

$$\Sigma_{Na} = \frac{6.023\times10^{23}}{23}\sigma_{Na}m_{Na} \quad , \tag{30}$$

where

6.023E+23 = Avogadro's number,
23 = atomic weight of sodium,
σ_{Na} = the thermal-neutron microscopic cross-section of ^{23}Na (0.534E−24 cm^2), and
m_{Na} = the mass of ^{23}Na per cubic centimeter of the solution in the phantom.

The total absorption cross-section (Σ_t) is calculated from the elemental abundance in the standard man and is equal to 0.02339 cm^{-1}.[19] Since the ratio of Σ_{Na}/Σ_t is proportional to the ^{23}Na concentration according to Eq. (30), it is convenient to give specific ^{24}Na activity in terms of Bq ^{24}Na/g ^{23}Na, which is essentially independent of the ^{23}Na concentration in the blood of an individual. Thus, Eq. (29) also can be expressed as

$$A = \lambda\left(\frac{\Sigma_{Na}}{m_{Na}\Sigma_t}\right)\frac{S}{V}\int_0^\infty \xi(E)\,\phi(E)\,dE \quad \mu Ci\,^{24}Na/g\,^{23}Na \quad . \tag{31}$$

Using the shape and size of the BOMAB phantom, for neutron radiation normally incident upon the front, the projected area (S) of body normal to the incident neutron beam is 5690 cm^2. The total volume (V) of the body is 68.28 × 10^3 cm^3. The relation between neutron fluence and blood activation is given by

$$A = 6.7\times10^{-7}\int_0^\infty \xi(E)\,\phi(E)\,dE \quad Bq\,^{24}Na/g\,^{23}Na \quad . \tag{32}$$

4.3.2 Fluence-to-Neutron Dose Conversion Factor

Before discussing fluence-to-dose conversion factors, it is important and necessary to state the meaning of the "dose" used in this research. There are several kinds of "dose" used in accident dosimetry. One is the surface-absorbed dose. This is the absorbed dose from neutrons interacting close to the surface of the body where the neutrons are incident.[1] This concept has the convenience of being consistent with the one used for the routine interpretation of the badge dosimeters. Another is the depth dose. This is the absorbed dose at the depth where the maximum radiation damage could occur.[23] Surface-absorbed doses are categorized according to

two reactions: 1) surface-absorbed heavy-charged particle [recoils and $^{14}N(n,p)^{14}C$] dose, and 2) surface-absorbed $^{1}H(n,\gamma)^{2}D$ dose. The variation of surface-absorbed dose and depth dose with incident neutron energy is given in Fig. 15. At energies above 0.1 MeV, the surface-absorbed dose comes mainly from recoils and heavy-charged particles; below 0.01 MeV, most comes from gamma rays produced by capture in hydrogen. Since the surface-absorbed dose from fast neutrons is of primary concern, it is customary to express the surface-absorbed dose using surface-absorbed recoil dose. The neutron fluence-to-dose conversion factors for depth and surface-absorbed doses are listed in Table 13.

4.3.3 Sodium-24 Activity-to-Dose Conversion Factors For Different Spectra

The total neutron dose received by the person per specific activity of ^{24}Na due to a fluence is given by

$$\frac{D}{A} = \frac{\int_0^\infty R(E)\,\phi(E)\,dE}{\lambda\left(\frac{\Sigma_{Na}}{m_{Na}\Sigma_t}\right)\left(\frac{S}{V}\right)\int_0^\infty \xi(E)\,\phi(E)\,dE} \quad . \tag{33}$$

The equation used for computer calculations is of the form,

$$\frac{D}{A} = \frac{\sum_1^K R(E_i)\,\phi(E_i)\,(E_{i+1}-E_i)}{6.7\times10^{-7}\sum_1^N \xi(E_j)\,\phi(E_j)\,(E_{j+1}-E_j)} \quad \frac{Gy}{Bq^{24}Na/g^{23}Na} \quad , \tag{34}$$

where $R(E_i)$ is the fluence-to-dose conversion factor.

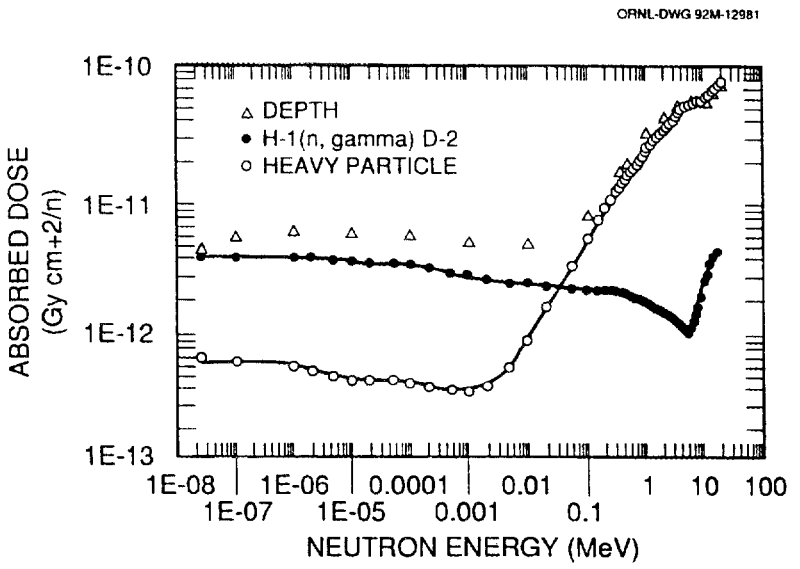

Fig. 15. Variations of surface-absorbed dose and depth dose with incident neutron energy.

Table 13. Neutron fluence-to-dose conversion factors

Neutron energy (MeV)	Surface-absorbed dose per unit fluence ($pGy.cm^2.n^{-1}$)		Depth-absorbed dose per unit fluence ($pGy.cm^2.n^{-1}$)
	Heavy particle	$^1H(n,\gamma)^2D$	
2.5E-8	0.600	3.9	4.65
1.0E-7	0.560	3.9	5.79
1.0E-6	0.520	3.9	6.31
2.0E-6	0.475	3.8	
5.0E-6	0.435	3.7	
1.0E-5	0.420	3.6	6.04
2.0E-5	0.420	3.5	
5.0E-5	0.410	3.5	
1.0E-4	0.380	3.4	5.79
2.0E-4	0.365	3.2	
5.0E-4	0.340	2.9	
1.0E-3	0.330	2.8	5.14
2.0E-3	0.360	2.6	
5.0E-3	0.520	2.4	
1.0E-2	0.840	2.4	4.96
2.0E-2	1.510	2.3	
5.0E-2	3.200	2.2	
1.0E-1	5.500	2.1	7.82
1.5E-1	7.500	2.1	
2.0E-1	9.000	2.1	
2.5E-1	10.40	2.1	
3.0E-1	11.80	2.1	
3.5E-1	13.40	2.1	
4.0E-1	15.50	2.0	
4.5E-1	16.80	2.0	
5.0E-1	16.00	2.0	18.0
5.5E-1	16.60	1.9	
6.0E-1	17.60	1.9	
7.0E-1	19.20	1.8	
8.0E-1	21.00	1.8	

Table 13. (continued)

Neutron energy (MeV)	Surface-absorbed dose per unit fluence ($pGy.cm^2.n^{-1}$)		Depth-absorbed dose per unit fluence ($pGy.cm^2.n^{-1}$)
	Heavy particle	$^1H(n,\gamma)^2D$	
9.0E-1	23.10	1.7	
1.0E-0	28.50	1.65	30.8
1.1	26.40	1.6	
1.5	29.70	1.50	
1.6	30.60	1.47	
1.8	32.40	1.43	
2.8	40.10	1.25	
3.0	43.00	1.22	
3.2	47.00	1.18	
3.4	49.80	1.15	
3.6	51.20	1.12	
3.8	51.50	1.09	
4.0	51.80	1.06	
4.5	51.70	1.01	
5.0	54.70	1.00	52.4
5.5	53.20	1.01	
6.0	54.70	1.05	
6.5	55.10	1.12	
7.0	55.90	1.24	
7.5	55.80	1.38	
8.0	54.80	1.56	
9.0	54.80	1.96	
10.0	55.80	1.45	60
11.0	58.60	2.76	
12.0	61.80	3.10	
13.0	64.60	3.40	
14.0	69.10	3.70	
15.0	73.30	3.89	
18.0	77.00	4.00	71.2

The calculated ^{24}Na activity-to-depth dose conversion factors and activity-to-surface absorbed dose conversion factors are listed in Tables 14 and 15, respectively. The conversion factors are expressed in units of Bq $^{24}Na/g$ ^{23}Na per Gy which is independent of the ^{23}Na concentration in blood. The activity-to-surface absorbed recoil dose conversion factors vary widely with a factor of 30 for the different spectra. A factor of 9 is associated with the variation of activity-to-depth dose conversion factors. These conversion factors are only valid for the neutrons incident on the front or back of the individual. The calculated blood activity-to-dose conversion factor for an uncollided fission spectrum is compared with the results calculated by several other authors in Table 16.

The person's orientation can be determined from sample-specific activity of hair. Four hair samples are taken from the front, back, left, and right of the head. The hair sample taken from the side facing the incident neutrons has the highest specific ^{32}P activity. The correction of the lateral irradiation to the blood activation will be discussed in Sect. 4.5.

The procedures to calculate the total neutron dose based on Tables 14 and 15 are simple if the following information is required:

1. the form of the fission material (e.g., metal or solution);
2. the type of shielding material (e.g., iron, lead, concrete, or graphite);
3. the thickness of the shielding; and
4. the type of moderator.

According to this information, an actual accident spectrum can be quickly approximated from 98 neutron spectra. Thus, the needed activity-to-dose conversion factor can be selected from Tables 14 or 15, depending on what kind of dose is used. The measured activity of ^{24}Na in blood is then divided by that factor to obtain the approximate total neutron dose that the person received.

4.4 ESTIMATION OF ACCIDENT NEUTRON DOSE USING BLOOD AND HAIR ACTIVATION

If some of the required information above is not available, the activity-to-dose conversion factor cannot be simply picked. Since the activity of ^{24}Na in blood is a function of neutron energies from thermal to fast, and activation of ^{32}P in hair is predominately determined by fast neutrons, the ratio of the measured activities between ^{32}P in hair and ^{24}Na in blood ($A_{P\text{-}32}/A_{Na\text{-}24}$) can provide additional information about the accident spectrum. Ninety-eight spectra were analyzed. Each spectrum is associated with its calculated activity ratio ($A_{P\text{-}32}/A_{Na\text{-}24}$).

Table 14. Activity-to-depth dose conversion factors for 98 neutron spectra

Spectrum description	Bq ^{24}Na/g ^{23}Na/Gy
Uncollided fission spectra	4420.978
Fissile solution, 2-cm-radius sphere, H_2O	5286.203
Fissile solution, 5-cm-radius sphere, H_2O	6371.074
Fissile solution, 10-cm-radius sphere, H_2O	6831.448
Fissile solution, 30-cm-radius sphere, H_2O	7007.752
Fissile solution, 50-cm-radius sphere, H_2O	7065.084
Fissile solution, 2-cm-radius sphere, D_2O	5054.450
Fission solution, 30-cm-radius sphere, D_2O	12,508.890
Fissile solution, 50-cm-radius sphere, D_2O	13,104.870
Unshielded HPRR spectra	9490.464
Concrete-shielded HPRR at 3 m	18,035.550
Plexiglas™-shielded HPRR spectra	9503.471
Steel-shielded HPRR at 3 m	13,115.560
Fission through 5-cm H_2O	7,159.78
Fission through 10-cm H_2O	5,946.788
Fission through 30-cm H_2O	5,217.638
Fission through 50-cm H_2O	4,598.610
Fission through 2-cm H_2O at surface	6,254.362
Fission through 2-cm D_2O	5,352.897
Fission through 5-cm D_2O	11,921.240
Fission through 10-cm D_2O	19,591.300
Fission through 30-cm D_2O	22,232.200
Fission through 2-cm D_2O at surface	5,699.753
Fission through 5-cm graphite	4,443.200
Fission through 10-cm graphite	5,045.371
Fission through 20-cm graphite	7,527.889
Fission through 40-cm graphite	15,289.580
Fission through 60-cm graphite	21,070.560
Fission through 10-cm polyethylene	8,187.709
Fission through 20-cm polyethylene	7,874.437
Fission through 40-cm polyethylene	6,786.181
Fission through 60-cm polyethylene	6,171.577
Fission through 5 cm of 1% borated polyethylene	6,786.258
Fission through 10 cm of 1% borated polyethylene	7,024.979
Fission through 20 cm of 1% borated polyethylene	6,424.929
Fission through 40 cm of 1% borated polyethylene	5,555.607
Fission through 60 cm of 1% borated polyethylene	5,137.284
Fission through 2.5 cm of 1% beryllium	4,682.685
Fission through 5-cm beryllium	5,433.610
Fission through 10-cm beryllium	8,245.635
Fission through 20-cm beryllium	14,805.380
Fission through 30-cm beryllium	19,423.520
Fission through 2.5-cm aluminum	4,343.166
Fission through 10-cm aluminum	4,991.291
Fission through 20-cm aluminum	6,897.882
Fission through 40-cm aluminum	15,007.160
Fission through 10-cm concrete	6,937.708
Fission through 20-cm concrete	9,762.745
Fission through 30-cm concrete	11,487.710

Table 14 (continued)

Spectrum description	Bq ^{24}Na/g ^{23}Na/Gy
Fission through 40-cm concrete	11,469.010
Fission through 60-cm concrete	10,225.530
Fission through 5-cm concrete with 10% iron	4,947.330
Fission through 10-cm concrete with 10% iron	6,303.580
Fission through 20-cm concrete with 10% iron	9,146.028
Fission through 60-cm concrete with 10% iron	12,905.100
Fission through 100-cm concrete with 10% iron	13,676.610
Fission through 5-cm concrete with 50% iron	5,002.999
Fission through 10-cm concrete with 50% iron	6,518.883
Fission through 20-cm concrete with 50% iron	10,073.380
Fission through 60-cm concrete with 50% iron	15,685.840
Fission through 100-cm concrete with 50% iron	17,000.240
Fission through 100 cm of 100% iron	33,927.420
Fission through 5-cm iron	5,469.457
Fission through 10-cm iron	6,787.291
Fission through 20-cm iron	10,322.110
Fission through 30-cm iron	13,888.670
Fission through 50-cm iron	19,691.580
Fission through 5-cm copper	6,116.939
Fission through 10-cm lead	5,479.682
Fission through 20-cm lead	7,017.728
Fission through 30-cm lead	8,931.132
Fission through 50-cm lead	13,744.390
Fission through 5-cm uranium-238	6,460.012
Fission through 10-cm uranium-238	9,044.037
Fission through 20-cm uranium-238	14,618.130
Fission through 30-cm uranium-238	19,482.460
Fission, H_2O-moderated through 2.5-cm beryllium	9,065.461
Fission, H_2O-moderated through 5-cm beryllium	9,762.268
Fission, H_2O-moderated through 10-cm beryllium	12,208.990
Fission, H_2O-moderated through 20-cm beryllium	17,438.060
Fission, H_2O-moderated through 10-cm aluminum	11,949.530
Fission, H_2O-moderated through 20-cm aluminum	16,596.360
Fission, H_2O-moderated through 10-cm concrete	11,282.060
Fission, H_2O-moderated through 20-cm concrete	12,695.320
Fission, H_2O-moderated through 30-cm concrete	12,228.920
Fission, H_2O-moderated through 20-cm iron	14,657.410
Fission, H_2O-moderated through 50-cm iron	22,951.940
Fission, H_2O-moderated through 5-cm copper	11,421.990
Fission, H_2O-moderated through 10-cm copper	13,541.040
Fission, H_2O-moderated through 20-cm copper	18,630.720
Fission, H_2O-moderated through 30-cm copper	23,819.060
Fission, H_2O-moderated through 50-cm copper	31,400.100
Fission, H_2O-moderated through 5-cm lead	10,261.460
Fission, H_2O-moderated through 10-cm lead	11,086.650
Fission, H_2O-moderated through 30-cm lead	15,391.080
Fission, H_2O-moderated through 50-cm lead	20,117.650
Cf-252, bare	4,252.925
Cf-252, D_2O-moderated	16,498.450

Table 15. Activity-to-surface absorbed recoil dose conversion factors for 98 neutron spectra

Spectrum description	Bq $^{24}Na/g$ $^{23}Na/Gy$
Uncollided fission spectra	5,148.012
Fissile solution, 2-cm-radius sphere, H_2O	6,268.756
Fissile solution, 5-cm-radius sphere, H_2O	7,745.387
Fissile solution, 10-cm-radius sphere, H_2O	8,434.567
Fissile solution, 30-cm-radius sphere, H_2O	8,691.078
Fissile solution, 50-cm-radius sphere, H_2O	8,747.739
Fissile solution, 2-cm-radius sphere, D_2O	5,958.232
Fission solution, 30-cm-radius sphere, D_2O	18,022.190
Fissile solution, 50-cm-radius sphere, D_2O	19,256.370
Unshielded HPRR spectra	12,442.130
Concrete-shielded HPRR at 3 m	34,020.150
Plexiglas™-shielded HPRR spectra	12,620.980
Steel-shielded HPRR at 3 m	18,239.440
Fission through 5-cm H_2O	8,933.494
Fission through 10-cm H_2O	7,217.911
Fission through 30-cm H_2O	6,200.282
Fission through 50-cm H_2O	5,289.228
Fission through 2-cm H_2O at surface	7,571.469
Fission through 2-cm D_2O	6,321.900
Fission through 5-cm D_2O	16,816.540
Fission through 10-cm D_2O	37,422.590
Fission through 30-cm D_2O	49,223.230
Fission through 2-cm D_2O at surface	6,759.996
Fission through 5-cm graphite	5,144.710
Fission through 10-cm graphite	5,882.466
Fission through 20-cm graphite	9,223.596
Fission through 40-cm graphite	24,428.670
Fission through 60-cm graphite	49,401.350
Fission through 10-cm polyethylene	10,639.690
Fission through 20-cm polyethylene	10,191.410
Fission through 40-cm polyethylene	8,415.736
Fission through 60-cm polyethylene	7,481.148
Fission through 5 cm of 1% borated polyethylene	8,335.457
Fission through 10 cm of 1% borated polyethylene	8,689.076
Fission through 20 cm of 1% borated polyethylene	7,791.646
Fission through 40 cm of 1% borated polyethylene	6,537.065
Fission through 60 cm of 1% borated polyethylene	5,963.723
Fission through 2.5 cm of 1% beryllium	5,422.227
Fission through 5-cm beryllium	6,336.179
Fission through 10-cm beryllium	10,224.060
Fission through 20-cm beryllium	23,297.520
Fission through 30-cm beryllium	42,553.450
Fission through 2.5-cm aluminum	5,020.561
Fission through 10-cm aluminum	5,787.836
Fission through 20-cm aluminum	8,181.982
Fission through 40-cm aluminum	21,306.470
Fission through 10-cm concrete	8,532.050
Fission through 20-cm concrete	13,021.600
Fission through 30-cm concrete	16,370.200

Table 15 (continued)

Spectrum description	Bq $^{24}Na/g$ $^{23}Na/Gy$
Fission through 40-cm concrete	16,443.170
Fission through 60-cm concrete	14,201.340
Fission through 5-cm concrete with 10% iron	5,824.183
Fission through 10-cm concrete with 10% iron	7,683.013
Fission through 20-cm concrete with 10% iron	12,205.230
Fission through 60-cm concrete with 10% iron	20,515.740
Fission through 100-cm concrete with 10% iron	22,821.450
Fission through 5-cm concrete with 50% iron	5,873.364
Fission through 10-cm concrete with 50% iron	7,915.741
Fission through 20-cm concrete with 50% iron	13,521.850
Fission through 60-cm concrete with 50% iron	26,108.610
Fission through 100-cm concrete with 50% iron	29,954.040
Fission through 100-cm of 100% iron	125,619.100
Fission through 5-cm iron	6,373.026
Fission through 10-cm iron	7,948.412
Fission through 20-cm iron	12,571.410
Fission through 30-cm iron	17,874.020
Fission through 50-cm iron	28,834.700
Fission through 5-cm copper	7,168.946
Fission through 10-cm lead	6,368.495
Fission through 20-cm lead	8,186.863
Fission through 30-cm lead	10,579.580
Fission through 50-cm lead	17,764.880
Fission through 5-cm uranium-238	7,617.407
Fission through 10-cm uranium-238	10,975.020
Fission through 20-cm uranium-238	19,362.940
Fission through 30-cm uranium-238	28,924.360
Fission, H_2O-moderated through 2.5-cm beryllium	11,873.140
Fission, H_2O-moderated through 5-cm beryllium	12,960.240
Fission, H_2O-moderated through 10-cm beryllium	17,498.190
Fission, H_2O-moderated through 20-cm beryllium	32,651.950
Fission, H_2O-moderated through 10-cm aluminum	17,160.640
Fission, H_2O-moderated through 20-cm aluminum	27,254.450
Fission, H_2O-moderated through 10-cm concrete	15,649.640
Fission, H_2O-moderated through 20-cm concrete	18,670.510
Fission, H_2O-moderated through 30-cm concrete	17,879.290
Fission, H_2O-moderated through 20-cm iron	20,277.420
Fission, H_2O-moderated through 50-cm iron	38,524.630
Fission, H_2O-moderated through 5-cm copper	15,409.010
Fission, H_2O-moderated through 10-cm copper	18,755.320
Fission, H_2O-moderated through 20-cm copper	28,566.050
Fission, H_2O-moderated through 30-cm copper	43,170.260
Fission, H_2O-moderated through 50-cm copper	86,896.260
Fission, H_2O-moderated through 5-cm lead	13,695.330
Fission, H_2O-moderated through 10-cm lead	14,938.340
Fission, H_2O-moderated through 30-cm lead	22,269.590
Fission, H_2O-moderated through 50-cm lead	33,147.250
Cf-252, bare	4,930.592
Cf-252, D_2O-moderated	27,688.800

Table 16. Blood activity-to-neutron dose conversion factor for fission neutrons calculated by different authors

Author	Spectrum	Phantom	Capture probability	Definition of neutron dose	Blood ^{24}Na–to–neutron dose conversion
Hankin[a] (LASL)	Jezebel	"Plastic man" in LASL	LASL's capture probability for 136–lb man	Fast neutron dose	About 3700 Bq ^{24}Na/g ^{23}Na/Gy
Cross[b]	Fission neutrons	"Standard" 70–kg man with 100-g ^{23}Na	Capture probability for a BOMAB phantom	Maximum total dose from a broad beam of fission neutrons	4199 Bq ^{24}Na/g ^{23}Na/Gy
Calculated in this research	Uncollided fission spectrum	BOMAB phantom	Capture probability for a BOMAB phantom	Maximum depth total neutron dose based on ICRP 21	4420 Bq ^{24}Na/g ^{23}Na/Gy
Hurst[c]	Fission neutrons	30–cm-diam cylinder	Hurst's capture probability	Fast neutron dose	1166 Bq ^{24}Na/g ^{23}Na/Gy

[a]See Reference No. 26.

[b]See Reference No. 27.

[c]See Reference No. 20.

Hair activation is calculated using the following equation

$$A_P = \frac{m\lambda G}{60 \times W} \int_{2.5MeV}^{\infty} \phi(E)\,\sigma(E)\,dE \quad Bq/g \quad , \tag{35}$$

where A_P is the specific activity of ^{32}P in hair, m is the sulfur content per gram of hair (45 mg/g hair), G is Avogadro's number (6.023E+23), W is the atomic weight of sulfur (32 g), $\sigma(E)$ is the activation cross-section of sulfur as a function of neutron energy, which is illustrated in Fig. 16, and λ is the decay constant for ^{32}P. The equation for calculating the ratio between blood and hair activities for each spectrum is

$$R = 7.14 \times 10^{23} \frac{\int_{2.5}^{\infty} \phi(E)\,\sigma(E)\,dE}{\int_{0}^{\infty} \xi(E)\,\phi(E)\,dE} \quad \frac{Bq^{32}P/g\ hair}{Bq^{24}Na/g^{23}Na} \quad . \tag{36}$$

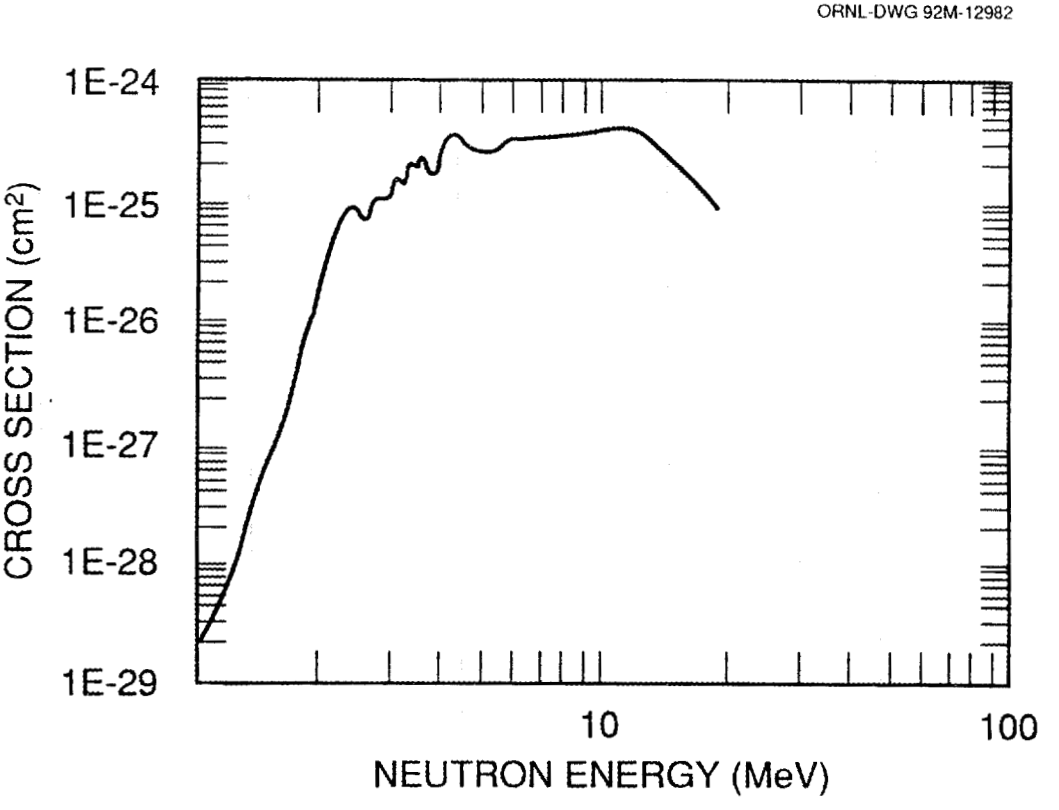

Fig. 16. Illustration of the cross-section of the $^{32}S(n,p)^{32}P$ reaction as a function of neutron energy.

The calculated activity ratios for 98 spectra are listed in Table 17. In addition, the ratio between fast neutron fluence (above 2.5 MeV) and total neutron fluence for each spectrum is also listed in Table 17. To relate the activity ratio to neutron dose, the activity ratios are plotted versus the blood-sodium activation per gray of dose (activity-to-dose conversion factors) in Fig. 17. The relationship between activity ratio and dose has an obvious trend in the range from 5.0E−5 to 1.0E−3 Bq ^{32}P/g hair/Bq^{24}Na/g^{23}Na, which covers the lightly shielded neutron spectra. The widely scattered points on the left side of the trend in Fig. 17 are from heavily shielded spectra. More detailed figures describing the relationship between dose and activity ratio for each type of shielding are presented in Figs. 18(a) to 18(d). Figure 18(a) shows the relation between dose and activity ratios from fission neutrons and fissile solution through different radii of H_2O, D_2O, and graphite. Figures 18(b) and 18(c) illustrate the relation from fission neutrons through different types of shielding. Figure 18(d) presents the relation from H_2O-moderated fission neutrons through different types of shielding.

The procedures to estimate neutron dose using these plots are simple if the ratios from the measured blood and hair activities fall in the range from 5.0E-5 to 1.0E-3 Bq ^{32}P/g hair per Bq ^{24}Na/g ^{23}Na. The blood activation is first read (Bq ^{24}Na/g ^{23}Na per Gy) from the trend on Fig. 17 at the point corresponding to the activity ratio (A_{P-32}/A_{Na-24}). The measured blood activity is then divided by that quantity to obtain the estimated neutron dose. This procedure is recommended when blood and hair activities are measured after an accident but other information related to the accident neutron source is not available. If the activity ratios fall in that range, other information such as the type of shielding material (lead, copper, etc.) is needed to estimate the dose from Figs. 18(a) to 18(d).

4.5 INTERPRETATION OF THE DERIVED NEUTRON DOSE

The activation of ^{24}Na in blood will be affected by the floor-scattering neutrons, the orientation of the individual, and the individual's size, in addition to the leakage neutron spectrum.

4.5.1 Floor-Scattering of Neutrons

Effects of floor-scattered neutrons on activation depend on the leakage spectrum, the distance between the assembly and the person, the height of the source, and the orientation of the person in the vertical plane if the neutrons are incident at the front of the body. Most of the scattered neutrons are thermalized and will contribute significantly to body activation, but they will contribute relatively little to the induced neutron dose. Thus, the estimated neutron dose based on data from Table 14 and from measured blood activity will be overestimated. Scattering correction factors for the 98 neutron spectra could be calculated for a particular geometry configuration at the time of an accident. In 1981, Cross[21] conducted experiments using a phantom irradiated by a fission neutron source at 3 m to see the scattering effect. The shift of the incident spectrum is shown in Fig. 19. The conclusion is that floor-scattered neutrons increase the activity produced by direct, frontally incident neutrons by a factor of 1.43.

Table 17. Ratio of activation of hair and blood and ratio of fluence above 2.5 MeV and total fluence for 98 neutron spectra

Spectrum description	Bq ^{32}P/g hair per Bq ^{24}Na/g ^{23}Na	$\phi^{Above\ 2.5\ Mev}/\phi^{Total}$
Uncollided fission spectra	0.229E-03	0.281E+00
Fissile solution, 2-cm-radius sphere, H_2O	0.186E-03	0.246E+00
Fissile solution, 5-cm-radius sphere, H_2O	0.152E-03	0.213E+00
Fissile solution, 10-cm-radius sphere, H_2O	0.141E-03	0.204E+00
Fissile solution, 30-cm-radius sphere, H_2O	0.142E-03	0.205E+00
Fissile solution, 50-cm-radius sphere, H_2O	0.139E-03	0.198E+00
Fissile solution, 2-cm-radius sphere, D_2O	0.198E-03	0.255E+00
Fission solution, 30-cm-radius sphere, D_2O	0.649E-04	0.110E+00
Fissile solution, 50-cm-radius sphere, D_2O	0.607E-04	0.103E+00
Unshielded HPRR spectra	0.700E-04	0.108E+00
Concrete-shielded HPRR at 3 m	0.207E-04	0.368E-01
Plexiglas™-shielded HPRR spectra	0.787E-04	0.122E+00
Steel-shielded HPRR at 3 m	0.218E-04	0.386E-01
Fission through 5-cm H_2O	0.144E-03	0.208E+00
Fission through 10-cm H_2O	0.206E-03	0.273E+00
Fission through 30-cm H_2O	0.272E-03	0.331E+00
Fission through 50-cm H_2O	0.397E-03	0.413E+00
Fission through 2-cm H_2O at surface	0.150E-03	0.211E+00
Fission through 2-cm D_2O	0.182E-03	0.238E+00
Fission through 5-cm D_2O	0.727E-04	0.122E+00
Fission through 10-cm D_2O	0.371E-04	0.676E-01
Fission through 30-cm D_2O	0.317E-04	0.564E-01
Fission through 2-cm D_2O at surface	0.166E-03	0.220E+00
Fission through 5-cm graphite	0.245E-03	0.288E+00
Fission through 10-cm graphite	0.197E-03	0.242E+00
Fission through 20-cm graphite	0.103E-03	0.146E+00
Fission through 40-cm graphite	0.284E-04	0.481E-01
Fission through 60-cm graphite	0.108E-04	0.184E-01
Fission through 10-cm polyethylene	0.137E-03	0.183E+00
Fission through 20-cm polyethylene	0.163E-03	0.201E+00
Fission through 40-cm polyethylene	0.228E-03	0.259E+00
Fission through 60-cm polyethylene	0.275E-03	0.297E+00
Fission through 5 cm of 1% borated polyethylene	0.165E-03	0.221E+00
Fission through 10 cm of 1% borated polyethylene	0.170E-03	0.226E+00
Fission through 20 cm of 1% borated polyethylene	0.216E-03	0.269E+00
Fission through 40 cm of 1% borated polyethylene	0.299E-03	0.338E+00
Fission through 60 cm of 1% borated polyethylene	0.351E-03	0.376E+00
Fission through 2.5 cm of 1% beryllium	0.215E-03	0.257E+00
Fission through 5-cm beryllium	0.161E-03	0.201E+00
Fission through 10-cm beryllium	0.765E-04	0.112E+00
Fission through 20-cm beryllium	0.226E-04	0.396E-01
Fission through 30-cm beryllium	0.899E-05	0.162E-01
Fission through 2.5-cm aluminum	0.257E-03	0.298E+00
Fission through 10-cm aluminum	0.194E-03	0.234E+00
Fission through 20-cm aluminum	0.105E-03	0.139E+00
Fission through 40-cm aluminum	0.221E-04	0.361E-01
Fission through 10-cm concrete	0.120E-03	0.184E+00
Fission through 20-cm concrete	0.789E-04	0.136E+00
Fission through 30-cm concrete	0.582E-04	0.110E+00

Table 17. (continued)

Spectrum description	Bq ^{32}P/g hair per Bq ^{24}Na/g ^{23}Na	$\phi^{Above\ 2.5\ Mev}/\phi^{Total}$
Fission through 40-cm concrete	0.565E-04	0.108E+00
Fission through 60-cm concrete	0.593E-04	0.114E+00
Fission through 5-cm concrete with 10% iron	0.231E-03	0.286E+00
Fission through 10-cm concrete with 10% iron	0.171E-03	0.233E+00
Fission through 20-cm concrete with 10% iron	0.102E-03	0.155E+00
Fission through 60-cm concrete with 10% iron	0.547E-04	0.853E-01
Fission through 100-cm concrete with 10% iron	0.444E-04	0.686E-01
Fission through 5-cm concrete with 50% iron	0.217E-03	0.269E+00
Fission through 10-cm concrete with 50% iron	0.150E-03	0.205E+00
Fission through 20-cm concrete with 50% iron	0.764E-04	0.119E+00
Fission through 60-cm concrete with 50% iron	0.285E-04	0.504E-01
Fission through 100-cm concrete with 50% iron	0.212E-04	0.389E-01
Fission through 100 cm of 100% iron	0.854E-10	0.258E-06
Fission through 5-cm iron	0.126E-03	0.169E+00
Fission through 10-cm iron	0.678E-04	0.961E-01
Fission through 20-cm iron	0.184E-04	0.294E-01
Fission through 30-cm iron	0.475E-05	0.813E-02
Fission through 50-cm iron	0.256E-06	0.499E-03
Fission through 5-cm copper	0.110E-03	0.149E+00
Fission through 10-cm lead	0.106E-03	0.149E+00
Fission through 20-cm lead	0.394E-04	0.645E-01
Fission through 30-cm lead	0.132E-04	0.237E-01
Fission through 50-cm lead	0.185E-05	0.374E-02
Fission through 5-cm uranium-238	0.111E-03	0.149E+00
Fission through 10-cm uranium-238	0.538E-04	0.805E-01
Fission through 20-cm uranium-238	0.160E-04	0.248E-01
Fission through 30-cm uranium-238	0.630E-05	0.102E-01
Fission, H_2O-moderated through 2.5-cm beryllium	0.859E-04	0.127E+00
Fission, H_2O-moderated through 5-cm beryllium	0.695E-04	0.105E+00
Fission, H_2O-moderated through 10-cm beryllium	0.403E-04	0.648E-01
Fission, H_2O-moderated through 20-cm beryllium	0.146E-04	0.256E-01
Fission, H_2O-moderated through 10-cm aluminum	0.565E-04	0.892E-01
Fission, H_2O-moderated through 20-cm aluminum	0.267E-04	0.452E-01
Fission, H_2O-moderated through 10-cm concrete	0.688E-04	0.118E+00
Fission, H_2O-moderated through 20-cm concrete	0.589E-04	0.106E+00
Fission, H_2O-moderated through 30-cm concrete	0.593E-04	0.110E+00
Fission, H_2O-moderated through 20-cm iron	0.109E-04	0.190E-01
Fission, H_2O-moderated through 50-cm iron	0.540E-06	0.907E-03
Fission, H_2O-moderated through 5-cm copper	0.530E-04	0.855E-01
Fission, H_2O-moderated through 10-cm copper	0.277E-04	0.464E-01
Fission, H_20-moderated through 20-cm copper	0.738E-05	0.125E-01
Fission, H_2O-moderated through 30-cm copper	0.192E-05	0.369E-02
Fission, H_2O-moderated through 50-cm copper	0.116E-05	0.175E-02
Fission, H_2O-moderated through 5-cm lead	0.693E-04	0.112E+00
Fission, H_2O-moderated through 10-cm lead	0.466E-04	0.794E-01
Fission, H_2O-moderated through 30-cm lead	0.669E-05	0.135E-01
Fission, H_2O-moderated through 50-cm lead	0.833E-06	0.181E-02
Cf-252 bare	0.267E-03	0.312E+00
Cf-252 D_2O-moderated	0.490E-04	0.847E-01

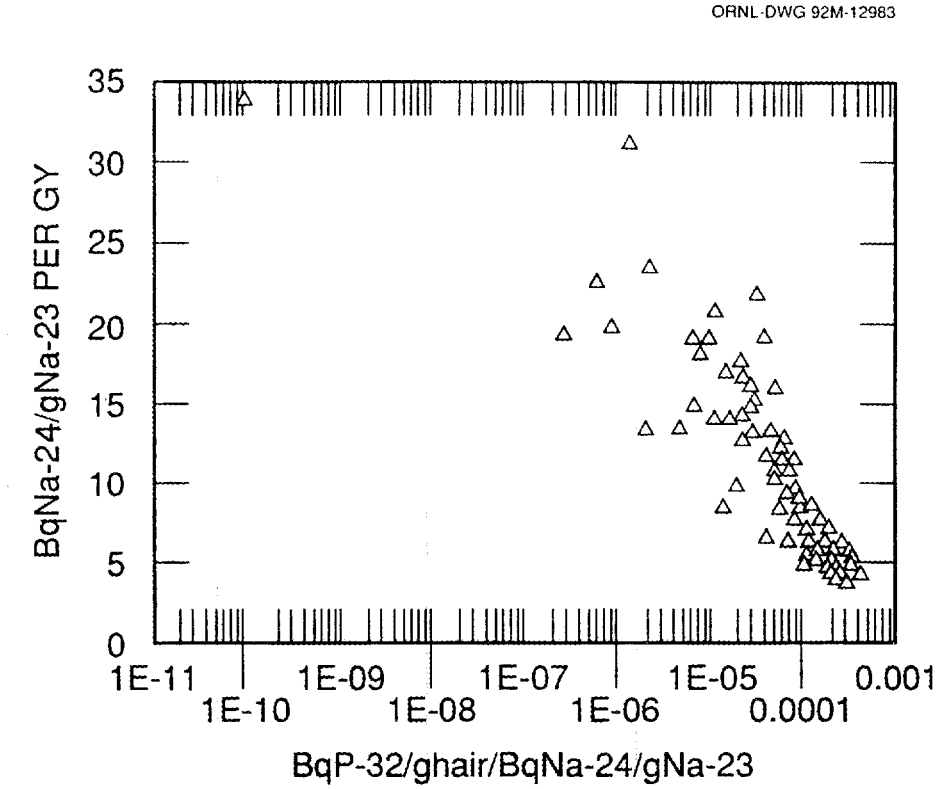

Fig. 17. Plots of activity-to-dose conversion factors using data on the specific activity of ^{24}Na in blood and ^{32}P in hair for 98 neutron spectrum descriptions.

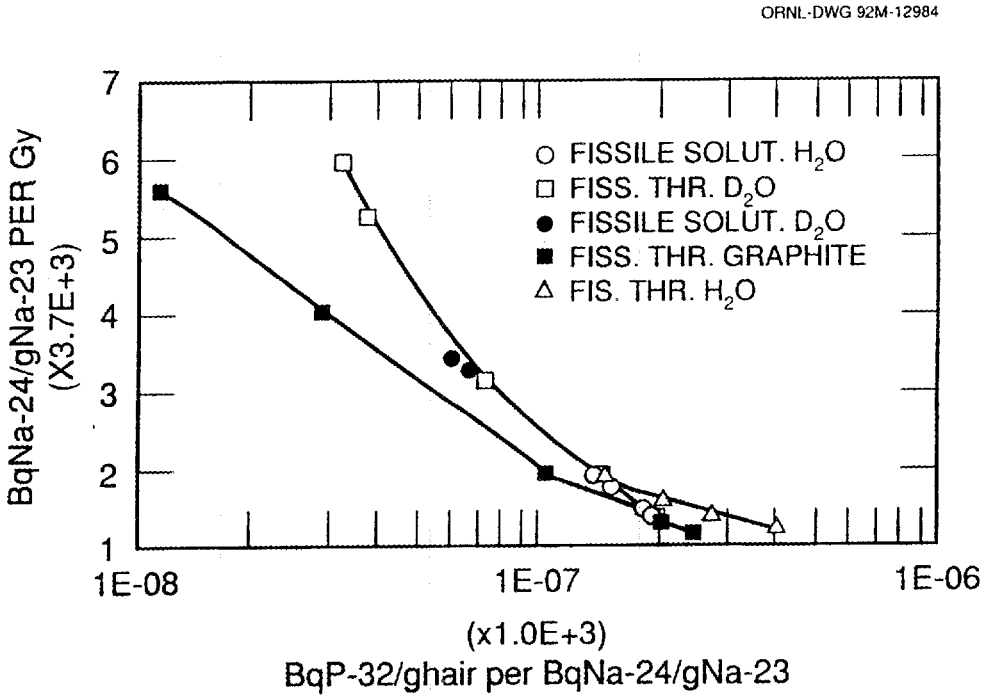

Fig. 18(a). Plots of activity-to-dose conversion factors using activity ratios for fission neutrons and fissile solution through different radii of H_2O, D_2O, and graphite.

ORNL-DWG 92M-12985

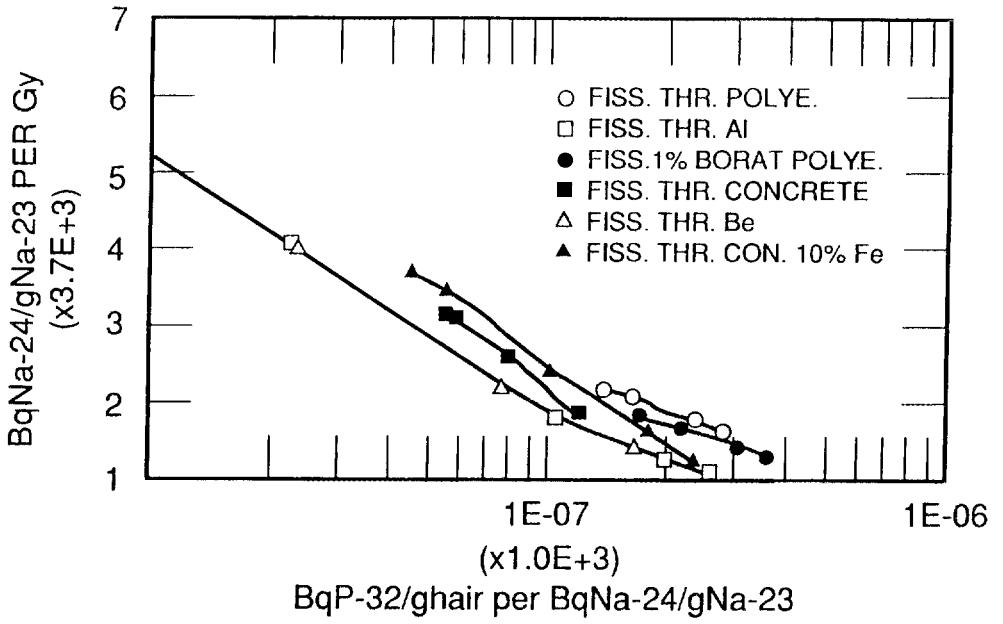

Fig. 18(b). Plots of activity-to-dose conversion factors using activity ratios for fission neutrons through different types of shielding.

ORNL-DWG 92M-12986

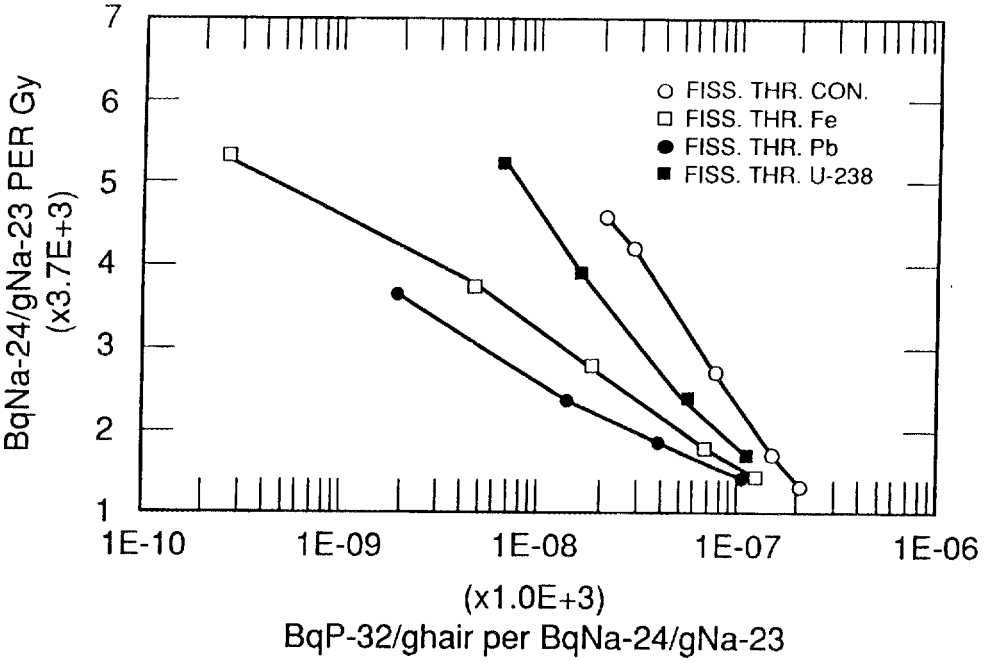

Fig. 18(c). Plots of activity-to-dose conversion factors using activity ratios for fission neutrons through different types of shielding.

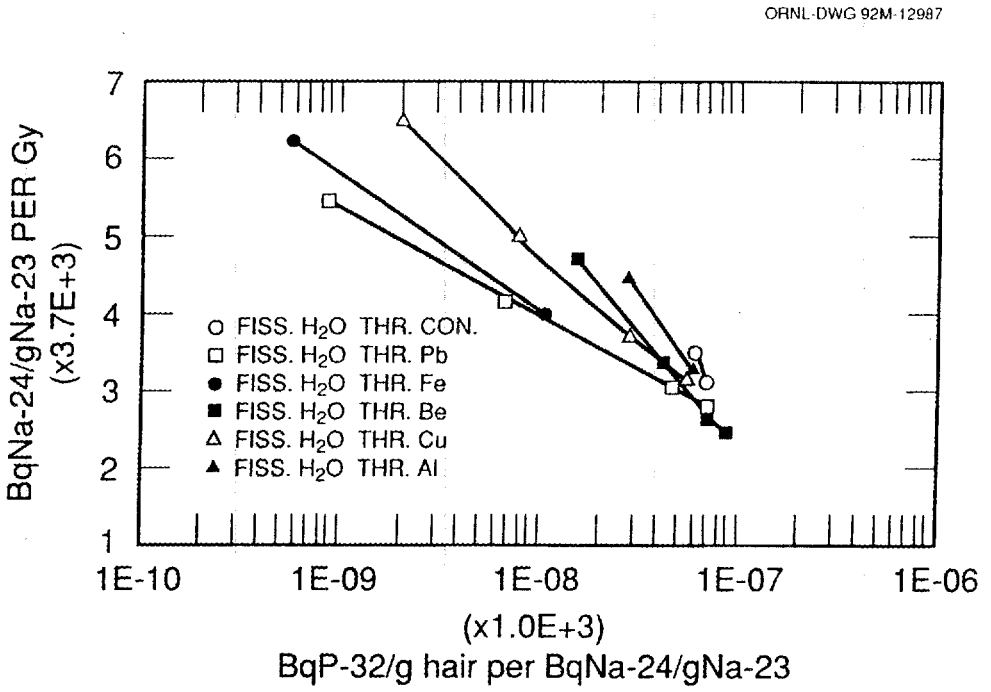

Fig. 18(d). Plots of activity-to-dose conversion factors using activity ratios for H_2O-moderated fission neutrons through different types of shielding.

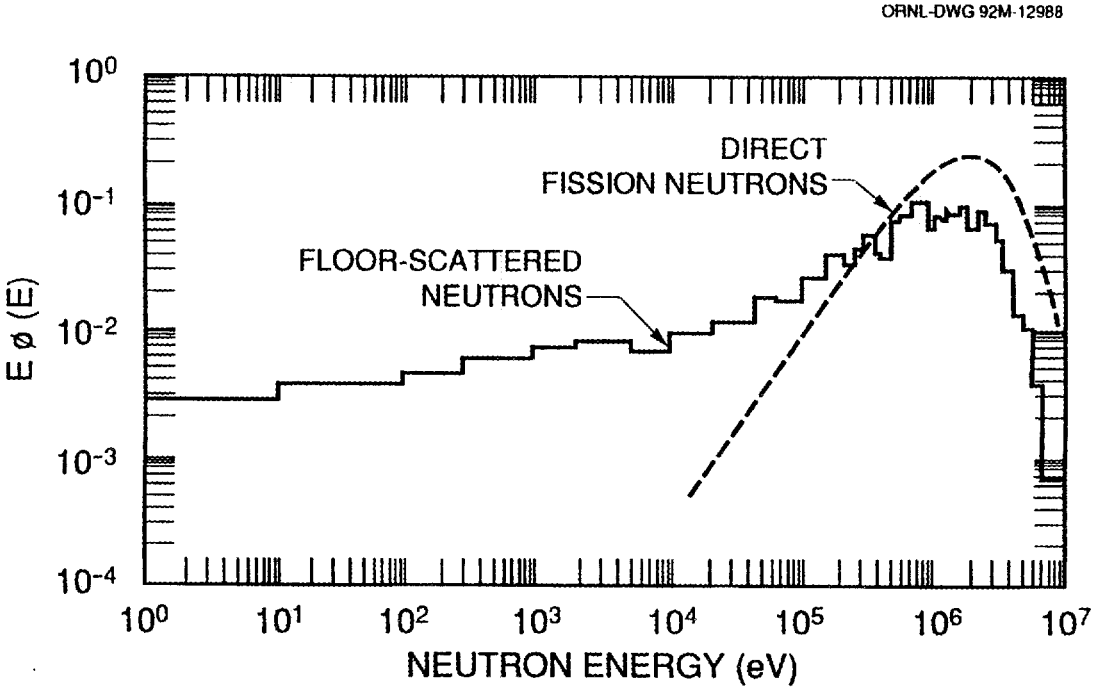

Fig. 19. Spectra of the "direct" and floor-scattered components of neutrons striking a phantom 3 m from a fission source. The source is 1.5 m above the floor (Cross, 1981).

4.5.2 Orientation of the Individual in the Moment of Excursion

Orientation affects body activation in two ways. Firstly, the direction of irradiation (that is, frontally or laterally) causes a different geometric factor (S/V) (see Eq. 29) because 2.04 times as many neutrons strike a BOMAB phantom from the front as from the side. Secondly, capture probabilities are different for neutrons incident on the front of a phantom than for neutrons incident on the side. The calculated results using the Monte Carlo method shows that the capture probability is about 20% greater for frontal irradiation than for lateral irradiation.[21] Thus, most of the variation caused by a person's orientation arises from the geometric factor rather than the capture probability.

If the person is irradiated laterally (determined from hair samples) in an accident, the measured blood activity should be multiplied by a factor of two before using the activity-to-dose conversion factors in Tables 14 or 15 to determine the total neutron dose received.

4.5.3 Human Size

If the person's size is larger than the BOMAB phantom, the capture probabilities should be increased because the large volume will provide more opportunities for neutrons to be absorbed. However, the specific activity is not significantly increased because the smaller surface-area-to-volume ratio nearly compensates for the larger capture probability.[21] Consequently, the body size does not contribute significantly to the variation in body activation.

5. CONCLUSIONS

5.1 CONCLUSIONS

Measurement procedures for activation of ^{24}Na in blood and ^{32}P in hair for the accident dosimetry system at ORNL have been established. The measurement procedure for blood is presented in Appendix A. The measurement procedure for hair is stated in Appendix B. Following an accident, these procedures could be followed to quickly provide the activation information within 2-6 h.

If an HPGe detector is used for counting 20-mL saline samples, a sensitivity of 0.01-0.02 Gy of total neutron dose for hard spectra and less than 0.005 Gy for soft spectra is obtained in a 30- to 60-min count.

A procedure to directly count hair samples using a liquid scintillation detector was established. About 0.06-0.1 Gy of total neutron dose can be measured from a 1-g hair sample using this measurement procedure. The simplicity of the analytical method, the small sample required (0.1-1.0 g), and the lower MDA make the established measurement procedure a practical approach for the determination of ^{32}P activity in hair induced by criticality accidents.

The established neutron dose assessment system for blood and hair is based on a collection of 98 neutron spectra. It does not require the large amount of information necessary for other types of personnel dosimetry. It also permits an estimate of the individual's neutron dose to be made within a few hours.

5.2 SUGGESTIONS FOR FUTURE WORK

An estimate of the neutron dose received by an individual should be obtained by different dosimetry techniques. It is very meaningful to calculate the TLD responses from 98 spectra and combine the results with the dosimetry system established by this research. Uncertainties associated with the established dose assessment system should be analyzed quantitatively. This would involve additional experiments and analyses.

REFERENCES

1. *Dosimetry for Criticality Accidents: A Manual*, Technical Report Series 211, Int. Atomic Energy Agency, Vienna, 1982.

2. G. E. Thoma, Jr., and N. Wald, "The Diagnosis and Management of Accidental Radiation Injury," *Journal of Occupational Medicine*, 423 (August 1959).

3. L. H. Hempelmann, H. Lisco, and J. G. Hoffman, *Ann. Int. Med.* **36**, 279 (1952).

4. R. V. Griffith, J. Palfalvi, and V. Maphvamath, *Compendium of Neutron Spectra and Detector Responses for Radiation Detection Purposes*, Technical Report Series 318, Int. Atomic Energy Agency, Vienna, 1990.

5. "Radiation Protection for Occupational Workers," DOE Order 5480.11 (1988).

6. Z. Ubovic and I. Miric, "Blood - Sodium Measurements for Nuclear Accident Dosimetry," *Advances in Radiation Protection Monitoring*, IAEA-SM-229/49, 1979.

7. "Operational Manual for HPGe Spectra Analyzer," EG&G ORTEC, Oak Ridge, Tenn., 1987.

8. "Certificate of Calibration of Mixed Radionuclide Gamma-Ray Reference Solution, M23529," Amersham Corporation, Arlington Heights, Ill., 1990.

9. W. S. Snyder and M. J. Cook, *Report of Task Group on Reference Man*, International Commission on Radiological Protection Publication 23, Oxford, 1975.

10. B. Altshuler and B. Pasternack, "Statistical Measures of the Lower Limit of Detection of a Radioactivity Counter," *Health Phys.* **9**, 293 (1963).

11. D. F. Peterson, V. E. Mitchell, and W. H. Langhman, "Estimation of Fast Neutron Doses in Man by $^{32}S(n,p)^{32}P$ Reaction in Body Hair," *Health Phys.* **6**, 1 (1961).

12. D. F. Peterson, *Personnel Dosimetry for Radiation Accidents*, Int. Atomic Energy Agency, Vienna, 1965.

13. D. E. Hankins, "Direct Counting of Hair Sample for ^{32}P Activation," *Health Phys.* **17**, 740 (1969).

14. *TRI-CARB Liquid Scintillation Analyzers*, 169-4019, Packard Instrument Company, Downers Grove, Ill., 1988.

15. *Operation Manual for TRI-CARB Liquid Scintillation Analyzers, Models 2000CA and 2000CA/LL*, 169-3029, Packard Instrument Company, Downers Grove, Ill., 1985.

16. D. L. Horrocks, *Applications of Liquid Scintillation Counting*, Academic Press, San Diego, Calif., 1974.

17. J. B. Birks, *The Theory and Practice of Scintillation Counting*, The MacMillan Company, New York, 1964.

18. Data base files from ORNL based upon Reference 25.

19. H. Ing and W. G. Cross, "Spectra and Dosimetry of Neutrons from Moderation of ^{235}U and ^{252}Cf Fission Sources In H_2," *Health Phys.* **29**, 839 (1975).

20. G. S. Hurst, R. H. Ritchie, and L. C. Emerson, "Accidental Radiation Protection Excursion at the Oak Ridge Y-12 Plant-III," *Health Phys.* **2**, 121 (1959).

21. W. G. Cross, "Neutron Activation of Sodium in Phantoms and the Human Body," *Health Phys.* **41**(1), 105 (1981).

22. F. W. Sanders and J. A. Auxier, "Neutron Activation of Sodium in Anthropomorphous Phantoms," *Health Phys.* **8** (1962).

23. International Commission on Radiological Protection, *Data for Protection against Ionizing Radiation from External Sources: Supplement to ICRP Publication 15*, ICRP Publication No. 21, Vienna, 1973.

24. D. I. Garber and R. R. Kinsey, *Neutron Cross Sections, Vol. II: Curves*, National Neutron Cross Section Center, Brookhaven National Laboratory, New York, 1976.

25. *Compendium of Neutron Spectra in Criticality Accident Dosimetry*, Technical Report Series 180, Int. Atomic Energy Agency, Vienna, 1978.

26. D. E. Hankins, *A Study of Selected Criticality-Dosimetry Methods*, LA-3910, Los Alamos Scientific Laboratory, 1968.

27. W. G. Cross, "Sodium Activation in the Human Body," *Radiation Prot Dosimetry* **10**, 1-4 (1985).

APPENDIX A:

Measurement Procedure for Activity of ^{24}Na in Blood

Measurement Procedure for Activity of ^{24}Na in Blood

1. Purpose

This procedure describes a method for the determination of ^{24}Na in human blood for estimation of the neutron dose as a result of a criticality accident.

2. Scope

In the event an individual is exposed to neutrons in a criticality accident, the induced activity of ^{24}Na in blood can be readily measured. This information can be used in conjunction with knowledge of the neutron spectrum to obtain an estimate of the neutron dose. Sodium-24 activity in blood can provide important information for the neutron dose evaluation.

3. Responsibility

A laboratory providing dose estimates from criticality accidents must maintain appropriate equipment, records, traceability of calibration sources, and computational methods support. In addition, it must demonstrate this capability by accurate determination of neutron-induced ^{24}Na activity in blind tests.

4. Summary of Methods

4.1 All information used for determining the accident neutron spectrum should be recorded, because the activation of blood sodium is a strong function of the energy distribution of the neutrons. The composition and location of all objects in the area is very useful for obtaining accurate information on the neutron spectrum. The victim's orientation is also important for correlation of dosimetry information with neutron dose and for determination of other parameters, such as projected area, used in dose calculations.

4.2 A minimum of 20 mL of blood should be obtained from the exposed individual by qualified medical personnel.

4.3 The gamma spectroscopy system selected in determination of induced activity should be evaluated in a QA program, and the applicable quality assurance tests of the equipment should be performed prior to measuring the induced ^{24}Na activity.

4.4 An efficiency calibration spectrum should be obtained for a liquid sample in the same geometry and volume as the sample from the exposed individual. A National Institute of Standards and Technology (NIST) traceable source should be used for calibration.

4.5 The counting time for measurement of ^{24}Na activity at the desired accuracy should be determined according to the required MDA. The equation for MDA (see Sect. 9.1 of Appendix A) is used.

4.6 A gamma-ray spectrum should be obtained from the sample of the exposed individual.

4.7 The 1.368-MeV photopeak counts should be used to calculate the induced ^{24}Na activity in the blood.

5. References

5.1 ICRP Report No. 23

5.2 NCRP Report No. 58

6. Materials and Equipment

The recommended gamma-ray spectroscopy system includes:

a. an HPGe detector with a liquid nitrogen cryostat;

b. detector bias supply, linear amplifier, MCA and data readout device;

c. gamma-ray spectroscopy data acquisition and analysis software;

d. a low-background shielding facility;

e. liquid gamma-ray standard source, traceable to NIST; and

f. 20-mL containers of the same geometry as the standard source.

7. Preparation of Detection System

The gamma-ray spectroscopy system will be checked according to QA procedures prior to use and all results should fall into the predetermined limits.

NOTE: The performance tests should include a system energy calibration, system count rate reproducibility, and system energy resolution. All performance testing should be conducted with a certified check source with energies spanning the 1368-keV photopeak.

8. Efficiency Calibration of Detection System

8.1 The liquid efficiency calibration source should be prepared with the same geometry and volume as the blood sample. Detailed techniques for quantitative sampling using a liquid standard source are discussed in Reference 2.

8.2 A gamma-ray spectrum should be obtained using the liquid calibration source at a desired and reproducible source-to-detector distance. It is desirable that 1000 net counts are accumulated in each full-energy gamma-ray peak used in the analysis.

8.3 The efficiency, E_{pi}, should be calculated as follows:

$$E_{pi} = \frac{C_{net}}{A_i \, I_i} \quad ,$$

where

E_{pi} = full-energy peak efficiency of each nuclide,

C_{net} = net gamma-ray count rate in the full-energy peak (counts/s live time),

A_i = gamma-ray emission rate at counting time (gamma rays/s), and

I_i = gamma-ray intensity at a certain energy for each nuclide.

8.4 The values for full-energy efficiency versus gamma-ray energy (E_{pi}) should be plotted on a log-log graph or fit to an appropriate mathematical function.

9. Measurement of the ^{24}Na Activity in Blood Sample

9.1 The proper counting time for blood samples should be determined by referring to the required MDA given in the following equation:

$$MDA = \frac{4.66\sqrt{C_B}}{60 \times T E_f V} \quad ,$$

where

MDA = required Minimum Detectable Activity (Bq/mL),

C_B = background counts,

T = counting time,

E_f = efficiency at interested energy peak, and

V = volume of blood sample (mL).

The specified MDA corresponds to a 95% statistical confidence level.

9.2 Blood samples from irradiated individuals should be properly identified.

9.3 The elapsed time between the accident excursion and collection of the blood sample should be documented.

9.4 The blood sample should be placed on the detector and measured at the source-to-detector distance used for efficiency calibration.

9.5 The gamma-ray spectrum should be accumulated and both the elapsed time from the end of irradiation to the start of counting and elapsed time from the end of irradiation to the end of counting should be recorded.

9.6 Counting times of 30 to 60 min may be required to obtain a LAUDE that corresponds to one of five lid doses for typical counting systems.

9.7 Net counts in the 1.368-MeV energy peak should be recorded.

10. Calculation of ^{24}Na Concentration in Blood Sample

The concentration of ^{24}Na in a blood sample and one standard deviation of the calculated activity are given by

$$A_{Na} = \frac{\lambda C_{Na} F_a}{60 \times (e^{-\lambda t_1} - e^{-\lambda t_2}) E_f I_\gamma V R_t}$$

and

$$\sigma_A = A_{Na} \sqrt{\frac{G_{B+C} + C_B}{C_{Net}^2}} \quad ,$$

where

A_{Na} = ^{24}Na concentration in a blood sample (Bq/mL),

C_{Net} = the number of net counts at 1.368-MeV energy peak,

λ = decay constant of ^{24}Na, 0.00077 min^{-1},

t_1 = elapsed time from the end of irradiation to the start of counting (min),

t_2 = elapsed time from the end of irradiation to the end of counting (min),

E_f = detection system efficiency at 1.368 MeV,

I_γ = gamma-ray intensity at 1.368 Mev, 100%,

V = total volume of blood sample (mL),

G_{B+C} = number of gross counts at 1.368 MeV,

C_B = number of background counts in the region corresponding to the peak area of G_c,

σ_A = one standard deviation of A,

R_t = metabolic correction factor, and

F_a = decay correction factor.

The correction for ^{24}Na radioactive decay is necessary if irradiation time is longer than one hour. The derived correction factor is

$$F_a = \frac{\lambda t_a}{1 - e^{-\lambda t_a}} \quad ,$$

where

F_a = decay correction factor,

λ = ^{24}Na decay constant, 0.00077 min^{-1}, and

t_a = irradiation time (min).

The metabolic half-life of ^{24}Na in the body is 12 d. If a correction is necessary, R_t can be taken to be

$$R_t = 4.87 e^{-0.0815 t} + 0.51 e^{-0.0513 t} + 0.0027 e^{-0.0015 t} \quad ,$$

where R_t is the fraction of the initial ^{24}Na remaining in the body at the time the sample is collected, and t is the number of days after the accident.

APPENDIX B:

Measurement Procedure for Activity of ^{32}P in Hair

Measurement Procedure for Activity of ^{32}P in Hair

1. Purpose

This procedure describes a method for determination of ^{32}P activity in human hair for estimation of neutron dose above 2.5 MeV from a nuclear criticality accident.

2. Scope

When an individual is exposed to neutrons, the induced activity of ^{32}P in hair can be readily measured. This information can be used in conjunction with knowledge of the neutron spectrum to obtain an estimate of the total neutron dose. The neutron dose above 2.5 MeV can be obtained directly from the ^{32}P activity measurement. The irradiated hair also provides information on the person's orientation in the accident.

3. Responsibility

A laboratory capable of providing dose estimates from criticality accidents must maintain appropriate equipment, records, traceability of calibration sources, and computational methods support. In addition, it must demonstrate this capability by accurate determination of neutron dose in blind tests.

4. Summary of Methods

4.1 All information associated with the accident that influences the neutron energy distribution should be recorded, including the location, orientation, shielding, and activity of the exposed personnel following the excursion. Composition and location of all objects in the area are used to obtain accurate information about the neutron spectrum.

4.2 Four hair samples from different areas of the head of the exposed person should be obtained, and a minimum of 0.1 g of hair is needed for each sample.

4.3 The liquid scintillation counting system selected for use to determine the induced activity should be evaluated in a QA program, and the applicable QA tests of the equipment should be checked for performance prior to measuring the induced ^{32}P activity.

4.4 If a NIST-traceable liquid ^{32}P source (or an equivalent maximum beta energy traceable liquid source) is available, an accurate efficiency calibration of the liquid scintillation counter can be obtained. If not, an efficiency tracing method may be used.

4.5 Hair samples should be dissolved or ashed to obtain the background measurement.

4.6 The counting time required for measuring ^{32}P activity should be based on the equation for MDA in Sect. 9.2 of Appendix B.

4.7 A ^{32}P net count rate should be obtained from the sample of the exposed individual, and the activity of ^{32}P should be calculated using the method in Sect. 9.2 of Appendix B.

5. Materials and Equipment

5.1 Liquid scintillation counter

5.2 Hair-dissolving materials

- 5.2.1 Hydrogen peroxide (30%)
- 5.2.2 Tissue solubilizer
- 5.2.3 Dithiothreitol (DTT)
- 5.2.4 Heater

5.3 Hair-ashing materials

- 5.3.1 High-temperature muffle furnace
- 5.3.2 Crucibles
- 5.3.3 Triton-10

5.4 Hair-cleaning materials

- 5.4.1 Detergent
- 5.4.2 Distilled water
- 5.4.3 Ethanol

5.5 Scintillation cocktail for biological materials, with high-efficiency and low chemiluminescence

5.6 Scintillation glass bottles (20 mL)

5.7 Analytical balance

5.8 Digital pipette and test tubes

6. Preparation of Hair Sample

6.1 Hair samples are taken from the front, back, left, and right of the victim's head and a name tag is placed on each sample.

6.2 The time of the accident, the elapsed time before the hair sample was taken, and the exact location on the head from which the sample was taken are documented.

6.3 The hair is washed with detergent, distilled water, and ethanol, and then dried in an oven with a temperature below 80°C.

6.4 The washed hair is cut as finely as possible. Care is taken not to mix the different samples.

6.5 Each sample is weighed accurately, and the weight is documented.

6.6 Hair Sample Treatment

Chemical dissolving or ashing may be used to prepare hair for liquid scintillation counting. The chemical dissolving method is recommended if the amount of hair in the sample is less than 0.3 g, otherwise the ashing method is used.

6.6.1 Chemical Dissolution of Hair

6.6.1.1 The weighted hair is placed into a scintillation glass vial. The following dissolving materials are added in order: 30% hydrogen peroxide, tissue solubilizer, and DTT. One gram of hair may require 14,000-μL tissue solubilizer, 7000-μL 30% hydrogen peroxide, and 0.12-g DTT.

6.6.1.2 The vial is swirled gently and digested at a constant temperature of 50°–60°C for 3–4 h until the hair is completely dissolved.

6.6.1.3 A 20-mL cocktail is placed in the vial for 20 min until the solution is transparent.

6.6.2 Ashing of Hair

6.6.2.1 The muffle furnace is preheated until the temperature is 800°C, usually for 1–2 h.

6.6.2.2 The weighted hair is placed in a crucible and the crucible is placed in the muffle furnace.

6.6.2.3 The temperature is kept at about 800°–815°C. Heating time is 15 min for 0.5 g and 20 min for 1 g.

6.6.2.4 The hot crucible is placed on a heat-isolating material for 20 min until the crucible cools.

6.6.2.5 All of the ashed powder is collected and placed in a scintillation glass vial. Five milliliters (5 mL) of cocktail is placed in the crucible; the solution is gently stirred and another 10 mL of cocktail is placed in the scintillation glass vial. If the glass vial can work under a high temperature (800°C), direct ashing of hair in a scintillation vial is recommended.

6.6.2.6 To get a relatively homogeneous sample, 5 mL of triton-10 is placed into the glass vial. The vial is capped and then shaken vigorously until the solution begins to gel. The vial is placed into the counting system.

7. Preparation of Background Sample

Similar procedures should be used for preparation of the background samples as used for the irradiated samples.

8. Measurement Procedures

8.1 It is recommended that the liquid scintillation counter be evaluated in a QA program. If not, conduct performance tests before using the counter. The tests should include the QIP/^{14}C efficiency check, ^{3}H efficiency check, and background check. The detailed procedures can refer to the operation manual of the counting system.

8.2 Perform an efficiency calibration if quenched ^{32}P liquid standards are available. When editing DPM protocol program, set counting time of interest, window 1 (energy region A) on 5-1710 keV, and window 2 (energy region B) on 50-1700 keV. Using the above procedures, the 95% efficiency can be directly used in the following counting and calculation instead of the efficiency calibration, which will reduce the preparation time and simplify the counting process with a reasonable accuracy.

8.3 Edit the protocol program.* Suggested inputs for the Packard 2000 are shown below.

Count time†	0, 60, or 90 min
# Counts/vial	1
# Vials/standard	1
# Vials/sample	1
1st vial background	Yes
Radionuclide	^{32}P
Region A: LL-UL	5.0-1700 keV
Region B: LL-UL	50.0-1700 keV
QIP	tSIE
ES terminator	Count
Data mode	CPM
Luminescence correction	On
Heterogeneity monitor	Yes
Printout	Count Time, CPMA, CPMB, 2S%, tSIE, SIS, and LUM%

8.4 Each sample is counted at least twice using the same procedure.

---

*Operational information for Packard Tri-Carb 2000CA and 2000CA/LL liquid scintillation systems.

†The count time of interest should meet the MDA.

9. Phosphorus-32 Activity Calculation

9.1 Induced ^{32}P activity in hair and one standard deviation of calculated activity are given by

$$A = \frac{C}{60 \times e^{-\lambda t} E_f m}, \quad (Bq/g),$$

and

$$\sigma_A = A\sqrt{\frac{G_c + B_c}{TC^2}},$$

where

A = ^{32}P activity induced in hair, dpm/g, or Bq/g,

C = CPM in energy region A (if the data in region A looks unreasonably large, the CPM in region B is used instead),

λ = ^{32}P decay constant,

t = elapsed time from the end of the accident until the start of counting,

E_f = counting efficiency for ^{32}P,

m = the amount of hair (g),

G_c = gross cpm in energy region A,

B_c = background cpm in energy region A,

σ_A = one standard deviation of A, and

T = counting time, which is the same for sample and background (min).

9.2 Minimum Detectable Activity

$$MDA = \frac{4.66\sqrt{B_c}}{60 \times E_f Tm}, \quad (Bq/g),$$

where

B_c	=	background (cpm),
T	=	counting time, which is same for sample and background (min),
E_f	=	counting efficiency,
m	=	the amount of hair sample (g), and
MDA	=	Minimum Detectable Activity (Bq/g) at a confidence level of 95%.

APPENDIX C.1:

FORTRAN Program for Interpolating 98 Neutron Spectra

FORTRAN PROGRAM FOR INTERPOLATING 98 NEUTRON SPECTRA

THIS PROGRAM INTERPOLATES 98 NEUTRON SPECTRA WITH THE SAME ENERGY BOUNDARIES. NECESSARY DATA FILES ARE: ENERGY OUTPUT FILE'S FILE NAME, FLUENCE OUTPUT FILE'S FILE NAME, NUMBER OF SPECTRA INTERPOLATED, INPUT ENERGY FILE'S FILE NAME, AND INPUT FLUENCE FILE'S FILE NAME.

```
      PROGRAM FOR INTERPOLATING THE FLUENCE
      CHARACTER*70 OUTE, OUTF, IENAME, IFNAME
     * ,ONAMEE, ONAMEF, NAMEE, NAMEF, NAMEOE, NAMEOF
      REAL  PHIU,E
      INTEGER I, J, COUNT,M,N,k,JJ
      DIMENSION EG(621), PHI(100), EAV(100)

      WRITE(*,*) 'ENERGY OUTPUT FILE_S FILE NAME'
      READ(*,'(A)') OUTE

      WRITE(*,*) 'FLUENCE OUTPUT FILE_S FILE NAME'
      READ(*,'(A)') OUTF

      WRITE(*,*) ' NUMBER OF FILES TO INTERPOLATED'
      READ(*,'(A)') NFILES

      WRITE(*,*) 'MIDDLE ENERGY FILE_S FILE NAME'
      READ (*, '(A)') IENAME

      WRITE(*,*) 'MIDDLE FLUENCE FILE_S FILE NAME'
      READ (*, '(A)') IFNAME

      OPEN(30, FILE=IENAME, STATUS='OLD')
      OPEN(40, FILE=IFNAME, STATUS='OLD')

      OPEN(16, FILE=OUTE, STATUS='OLD')
      OPEN(17, FILE=OUTF, STATUS='OLD')

      OPEN(12, FILE='ER621', STATUS='OLD')
      READ(12,*) EG

      DO JJ=1, NFILES

      READ(30,'(A)') NAMEE
      READ(40,'(A)') NAMEF
      OPEN(10,FILE=NAMEE,STATUS='OLD')
      OPEN(11,FILE=NAMEF,STATUS='OLD')

      READ(16,'(A)') NAMEOE
      READ(17,'(A)') NAMEOF
      OPEN(14, FILE=NAMEOE, STATUS='UNKNOWN')
      OPEN(15, FILE=NAMEOF, STATUS='UNKNOWN')

      I=1
      DO while (.TRUE.)
```

```
      READ(10, *, END=99) EAV(I)
      READ(11,*,END=99) PHI(I)
      I=I+1
      END DO
99    COUNT=I-1
      write(14,*) EAV(1)
      CLOSE (10)
      CLOSE(11)

      k=1
      DO 300 J=2, COUNT

      DO 400 I=k, 621
            IF (EG(I).GT.EAV(J-1) .AND. EG(I).LE.EAV(J)) THEN
 PHIU=PHI(J-1)+((PHI(J)-PHI(J-1))/(EAV(J)-EAV(J-1)))*
     >          (EG(I)-EAV(J-1))

       E=EG(I)
          WRITE(15,*) PHIU
       WRITE(14,*) E

      ELSE IF (EG(I).GT.EAV(J)) THEN
      GOTO 500
            ELSE
      END IF

400   CONTINUE

500   N=I+1
        K=N-1

300   CONTINUE

      END DO

      STOP
      END
```

APPENDIX C.2:

FORTRAN Program for Calculating Activity Ratio Between ^{32}P in Hair and ^{24}Na in Blood for 98 Neutron Spectra

FORTRAN PROGRAM FOR CALCULATING ACTIVITY RATIO BETWEEN ^{32}P IN HAIR AND ^{24}NA IN BLOOD FOR 98 NEUTRON SPECTRA

THIS PROGRAM CALCULATES THE ACTIVATION RATIO BETWEEN ^{32}P IN HAIR AND ^{24}NA IN BLOOD. NECESSARY DATA FILES ARE: NUMBER OF FILES TO BE INTERPOLATED, ENERGY BOUNDARY FILE'S FILE NAME, FLUENCE FILE'S FILE NAME, AND SPECTRUM NAME LIST.

```
      PROGRAM CONVERSION FACTOR CALCULATION
      CHARACTER*70, NAMEFF, NAMEFE,ICNAME,
*     ,ONAME,FENAME,FFNAME,DNAME
      REAL PHITOT, ANA1,A1,AP,SUMPHIU,
      INDEX1,FPHI,SUL_B,SUL_A,R,
     > ANA2,A2,INDEX2,ASIGMA,FFPHI
      INTEGER I,J,N,COUNT,K,JJ
      DIMENSION  EB(1000), PHIU(1000), EC(28), CAP(27),SIGMAP(155)
      DATA ASIGMA/240E-27/

      WRITE(*,*) 'OUTPUT FILE NAME'
      READ(*, '(A)') ONAME

      WRITE(*,*) 'NUMBER OF FILES TO BE CALCULATED '
      READ(*,*) NFILES

      WRITE(*,*) 'ENERGY BOUNDARY FILE_S FILE NAME'
      READ(*,'(A)') FENAME

      WRITE(*,*) 'FLUENCE FILE_S  FILE NAME'
      READ(*,'(A)') FFNAME

      WRITE(*,*) 'SPECTRUM NAME LIST'
      READ(*,'(A)') DNAME

      OPEN(30, FILE=FENAME,STATUS='OLD')
      OPEN(40,FILE=FFNAME,STATUS='OLD')
      OPEN(20, FILE=DNAME,STATUS='OLD')

      OPEN(12, FILE='UE28.PHA', STATUS='OLD')
      READ(12,*) EC

      OPEN(15,FILE='P32CS.25', STATUS='OLD')
      READ(15,*) SIGMAP

      OPEN(14,FILE='UCS27.PHA', STATUS='OLD')
      READ(14,*) CAP

      OPEN(13, FILE=ONAME, STATUS='NEW')

      DO JJ=1,NFILES
      READ(30,'(A20)') NAMEFE
      READ(40,'(A20)') NAMEFF
```

```
      READ(20,'(A70)') DNAME

      OPEN(10,FILE=NAMEFF, STATUS='OLD')
      OPEN(11,FILE=NAMEFE,STATUS='OLD')

      I=1
      DO 50 n=1,1000
      READ(11,*,END=99) EB(I)
      I=I+1

50    CONTINUE

99    COUNT=I-1

      J=1
      DO 60 I=1,1000
      READ(10,*,END=98) PHIU(J)
      J=J+1

60    CONTINUE

98    PHITOT=0
      DO 200 I=2, COUNT
            PHITOT=PHITOT+PHIU(I-1)*(LOG(EB(I))-
     >       LOG(EB(I-1)))

200   CONTINUE

      DO 300 I=1,COUNT
            IF(EB(I).EQ.2.5) THEN
            M=I+1
            ELSE
            END IF

300   CONTINUE

      AP=0
      ANA1=0
      A1=0
      FPHI=0
      J=M-1
      A2=0
      ANA2=0

      DO 400 I=M, COUNT

      AP=AP+(1.293E+10)*PHIU(I-1)*SIGMAP(I-J)*(LOG(EB(I))
     > -LOG(EB(I-1)))

      FPHI=FPHI+PHIU(I-1)*(LOG(EB(I))
     > -LOG(EB(I-1)))

400   CONTINUE
      R=FPHI/PHITOT
```

```
      N=1
      DO 5000 J=2,28
            SUMPHIU=0
      DO 4000 I=N,COUNT
            IF (EB(I-1).GE.EC(J-1).AND.EB(I-1).LT.EC(J)) THEN

            SUMPHIU=SUMPHIU+PHIU(I-1)*(LOG(EB(I))
     >        -LOG(EB(I-1)))

            ELSE IF (EB(I-1).GE.EC(J)) THEN
            GOTO 1000
            ELSE
            END IF

4000  CONTINUE

1000  N=I+1

      A1=CAP(J-1)*SUMPHIU*(1.81667E-8)
      ANA1=ANA1+A1
      ANA2=(ANA1/1.81667E-8)* (3.47E-14)

5000  CONTINUE

      INDEX1=AP/ANA1
      INDEX2=AP/ANA2
      FFPHI=AP/(1.293E+10 * ASIGMA)
      SUL_A=FFPHI/ANA1
      SUL_B=FPHI/ANA1

      WRITE(13,1) DNAME,INDEX1,INDEX2,R
1     FORMAT( A43, E9.3, 2X, E9.3, 2X, E9.3)

      END DO

      STOP
      END
```

APPENDIX C.3:

FORTRAN Program for Calculating Blood Activity-to-Dose Conversion Factors for 98 Neutron Spectra

FORTRAN PROGRAM FOR CALCULATING BLOOD ACTIVITY-TO-DOSE CONVERSION FACTORS FOR 98 NEUTRON SPECTRA

THIS PROGRAM CALCULATES BLOOD ACTIVITY-TO-DOSE CONVERSION FACTORS. NECESSARY DATA FILES ARE: NUMBER OF SPECTRA TO BE ANALYZED, ENERGY BOUNDARY FILE'S FILE NAME, FLUENCE FILE'S FILE NAME, AND SPECTRUM NAME LIST.

```
      PROGRAM  DOSE CONVERSION FACTOR CALCULATION

      CHARACTER*70, NAMEFF, NAMEFE,ICNAME,
     * ONAME,FENAME,FFNAME,DNAME
      REAL  K, PHISUM, PHITOT, ATOTAL,A,D,DTOTAL,SUMPHIU,W
      INTEGER I,J,N,COUNT,ICOUNT,JJ
      DIMENSION C(14), EB(1000), PHIU(1000), E(15), EC(28), CAP(27)
      DATA C/3.9E-10, 3.9E-10, 3.9E-10, 3.6E-10, 3.4E-10, 2.8E-10,
     *      2.4E-10, 2.1E-10, 2.0E-10, 1.65E-10, 1.4E-10,
     *        1.0e-10, 2.45E-10, 3.7E-10/
      DATA E/2.50E-8, 1.0E-7, 1.0E-6, 1.0E-5, 1.0E-4, 1.0E-3,
     *      1.0E-2, 1.0E-1, 5.0E-1, 1.0E+0, 2.0E+0,
     *        5.0E+0, 10.0E+0, 14.0E+0,20.0E+0/


      WRITE(*,*) 'OUTPUT FILE NAME'
      READ(*, '(A)') ONAME

      WRITE(*,*) 'NUMBER OF FILES TO BE CALCULATED'
      READ(*,*) NFILES

      WRITE(*,*) 'ENERGY BOUNDARY FILE_S FILE NAME'
      READ(*,'(A)') FENAME

      WRITE(*,*)'FLUENCE FILE_S FILE NAME'
      READ(*,'(A)') FFNAME

      WRITE(*,*) 'FILES_NAME LIST'
      READ(*,'(A)') DNAME

      OPEN(30, FILE=FENAME, STATUS='OLD')
      OPEN(40, FILE=FFNAME, STATUS='OLD')
      OPEN(20, FILE=DNAME, STATUS='OLD')

      OPEN(12, FILE='UE28.PHA', STATUS='OLD')
      READ(12,*) EC

      OPEN(14,FILE='UCS27.PHA', STATUS='OLD')
      READ(14,*) CAP

      OPEN(13, FILE=ONAME, STATUS='NEW')

      DO JJ=1,NFILES
```

```
      READ(30,'(A20)') NAMEFE
      READ(40,'(A20)') NAMEFF
      READ(20,'(A70)') DNAME

      OPEN(10, FILE=NAMEFF, STATUS='OLD')
      OPEN(11, FILE=NAMEFE, STATUS='OLD')

      I=1
      DO 50 n=1,1000
      READ(11,*,END=99) EB(I)
      I=I+1
50    CONTINUE

99    COUNT=I-1
      CLOSE (11)

      J=1
      DO 60 I=1,1000
      READ(10,*,END=98) PHIU(J)
      J=J+1
60    CONTINUE
      CLOSE(10)

98    PHITOT=0
      DO 300 I=2, COUNT
            PHITOT=PHITOT+PHIU(I-1)*(LOG(EB(I)*1000000)-
     >       LOG(EB(I-1)*1000000))
300   CONTINUE

      N=1
      DTOTAL=0
      K=0
      A=0
      D=0
      ATOTAL=0

      DO 500 J=2, 15

        PHISUM=0

        DO 400 I=N, COUNT

          IF (EB(I-1).GE.E(J-1).AND.EB(I-1).LT.E(J)) THEN
           PHISUM=PHISUM + PHIU(I-1)*(Log(EB(I)*1000000)
     >       -Log(EB(I-1)*1000000))

            ELSE IF (EB(I-1).GE.E(J)) THEN
          GOTO 100
          ELSE
          END IF

400     CONTINUE

100   N=I+1
```

```
        D=C(J-1)*PHISUM
        DTOTAL=DTOTAL+D
500     CONTINUE

        N=1
        DO 5000 J=2,28
                SUMPHIU=0
        DO 4000 I=N,COUNT
                IF (EB(I-1).GE.EC(J-1).AND.EB(I-1).LT.EC(J)) THEN
                SUMPHIU=SUMPHIU+PHIU(I-1)*(LOG(EB(I)*1000000)
     >         -LOG(EB(I-1)*1000000))
                ELSE IF (EB(I-1).GE.EC(J)) THEN
                GOTO 1000
                ELSE
                END IF

4000    CONTINUE

1000    N=I+1

        A=CAP(J-1)*SUMPHIU
        ATOTAL=ATOTAL+A

5000    CONTINUE

        K=1.81667E-8 * (ATOTAL/DTOTAL)
        W=2.90867E+13 *(DTOTAL/ATOTAL)

        WRITE(13,1) DNAME,K,W
1       FORMAT(A45,1X,F10.3,6X,F10.3)
        END DO

        STOP
        END
```

APPENDIX D:

Additional Bibliography

ADDITIONAL BIBLIOGRAPHY

1. J. E. Turner, *Atoms, Radiation, and Radiation Protection*, Pergamon Press, Inc, New York, 1986.

2. A. B. Brodsky, *CRC Handbook of Radiation Measurements and Protection, Section A, Volume I: Physical Science and Engineering Data*, CRC Press, Inc., West Palm Beach, Fl., 1978.

3. E. D. Bransome, Jr., *The Current Status of Liquid Scintillation Counting*, Grune & Stratton, Inc., New York, 1970.

4. H. J. M. Bowen and D. Gibbons, *Radiation Analysis*, Oxford at the Clarendon Press, New York, 1963.

5. *Neutron Monitoring for Radiation Protection Purposes*, Proceeding of a Symposium on Neutron Monitoring for Radiation Protection Purposes, Vol. I and Vol. II, Int. Atomic Energy Agency, Vienna, 1973.

6. *Selected Topics in Radiation Dosimetry*, Proceedings of the Symposium on Selected Topics in Radiation Dosimetry, Int. Atomic Energy Agency, Vienna, June 1960.

7. J. M. A. Lenihan, S. J. Thomson, and V. P. Guinn, *Advances in Activation Analysis*, Academic Press, Inc., Downers Grove, Ill., 1972.

8. J. B. Briks, *The Theory and Practice of Scintillation Counting*, A Pergamon Press Book, The Macmillan Company, New York, 1964.

9. *Neutron Monitoring for Radiation Protection Purposes*, Proceeding of a Symposium on Neutron Monitoring for Radiation Protection Purposes, Int. Atomic Energy Agency, Vienna, September 1966.

10. W. J. Gray and A. M. James, *Radiochemical Methods*, John Wiley & Sons, New York, 1986.

DISTRIBUTION

1. A. B. Ahmed
2. J. F. Alexander
3. B. A. Berven
4. J. S. Bogard
5. R. S. Bogard
6. K. J. Brown
7-10. W. H. Casson
11. S. W. Croslin
12. E. C. Crume
13. W. L. DeRossett
14. T. C. Dodd
15. C. M. Hopper
16. J. B. Hunt
17. G. D. Kerr
18. C. E. Maples
19. K. L. McMahan
20-24. G. T. Mei
25. W. F. Ohnesorge
26. P. S. Rohwer
27. C. S. Sims
28. M. Thein
29. Central Research Library
30. ORNL Technical Library, Y-12
31-32. Laboratory Records
33. Laboratory Records—RC
34. ORNL Patent Section

35. Office of Assistant Manager for Energy Research and Development, Department of Energy, Oak Ridge Operations, P.O. Box 2001, Oak Ridge, TN 37831-8600
36-37. Office of Scientific and Technical Information, P.O. Box 62, Oak Ridge, TN 37831
38. A. Bassett, Department of Energy, Oak Ridge Operations, P.O. Box 2008, Oak Ridge, TN 37831-6269
39. W. K. Crase, Westinghouse Savannah River Company, Savannah River Site, Bldg. 735A, Aiken, SC 29802
40. Y. Feng, SENES Oak Ridge, Inc., 677 Emory Valley Road, Suite C, Oak Ridge, TN 37830
41. J. F. Higginbotham, Radiation Center, Oregon State University, Corvallis, OR 97331
42. H. H. Hsu, Los Alamos National Laboratory, P.O. Box 1663, MS-G761, Los Alamos, NM 87545
43-44. L. F. Miller, University of Tennessee, Nuclear Engineering Department, 207 Pasqua Engineering Building, Knoxville, TN 37996-2300
45. J. W. Poston, Texas A&M University, Department of Nuclear Engineering, College Station, TX 77843
46. R. B. Schwartz, National Institute of Standards and Technology, Bldg. 235, Gaithersburg, MD 20899
47. G. G. Simons, Engineering Experiment Station, Durland Hall, Kansas State University, Manhattan, KS 66506-5103